Received: 18 January 2023 | Accepted: 28 April 2023

DOI: 10.1111/1365-2745.14136

Journal of Ecology | BRITISH ECOLOGICAL SOCIETY

RESEARCH ARTICLE

Drought intensity alters productivity, carbon allocation and plant nitrogen uptake in fast versus slow grassland communities

Natalie J. Oram[1,2] | Johannes Ingrisch[1] | Richard D. Bardgett[3] | Fiona Brennan[2] | Georg Dittmann[4] | Gerd Gleixner[4] | Paul Illmer[5] | Nadine Praeg[5] | Michael Bahn[1]

[1]Department of Ecology, University of Innsbruck, Innsbruck, Austria

[2]Environment, Soils and Land Use Department, Teagasc, Johnstown Castle, Ireland

[3]Department of Earth and Environmental Sciences, The University of Manchester, Manchester, UK

[4]Max Planck Institute for Biogeochemistry, Jena, Germany

[5]Department of Microbiology, University of Innsbruck, Innsbruck, Austria

Correspondence
Natalie J. Oram
Email: natalie.oram@uibk.ac.at

Johannes Ingrisch
Email: johannes.ingrisch@uibk.ac.at

Funding information
NJO has received funding from the Research Leaders 2025 programme co-funded by Teagasc and the European Union's Horizon 2020 research and innovation programme under the Marie Sklowdowska-Curie grant, Grant/Award Number: 754380; RDB acknowledges support from a European Research Council (ERC) Advanced Grant, Grant/Award Number: 883621; The experiment was also supported by a Tiroler Wissenschaftsfonds grant to JI, Grant/Award Number: F.16568/5-2019

Handling Editor: Biao Zhu

Abstract

1. Grasslands face more frequent and extreme droughts; yet, their responses to increasing drought intensity are poorly understood. Increasing drought intensity likely triggers abrupt shifts (thresholds) in grassland ecosystem functioning which can implicate recovery trajectories.
2. Here, we determined how drought intensity affects plant productivity, and plant–soil carbon (C) and nitrogen (N) cycling. We exposed model grassland plant communities with contrasting resource acquisition strategies (a fast- vs a slow-strategy plant community), to a gradient of drought intensity. The drought gradient ranged from well-watered to severely water-limited conditions. We identified thresholds of plant community productivity (above-ground biomass) at peak drought and 2 months after re-wetting, and measured net ecosystem exchange and ecosystem respiration of C throughout the drought and recovery phases. At peak drought and 1 week after re-wetting, we traced recently acquired C from plants to the soil and into microbial biomass and fatty acids using ^{13}C pulse labelling, and measured plant and soil N.
3. At peak drought, slow-strategy plant communities were more drought resistant than fast-strategy communities, as the threshold in plant productivity occurred at a higher drought intensity for the slow- than the fast-strategy community. Shortly after re-wetting, microbial uptake of recent plant-assimilated C increased with increasing past drought intensity, coinciding with an increase in soil N availability and leaf N. Threshold responses to drought intensity at peak drought translated into non-linear recovery responses, with greater compensatory growth in the fast-strategy community. At peak drought, increasing drought intensity reduced C uptake and increased relative C partitioning to leaves and microbial biomass. Upon re-wetting, plant community strategy mediated drought intensity effects

Natalie J. Oram and Johannes Ingrisch—Equal contribution.

on plant and soil C and N dynamics and plant recovery trajectories. The fast-strategy community recovered quickly, with higher leaf N than the slow community, while the slow community increased C allocation to microbial biomass.

4. *Synthesis*. Our findings highlight that C and N dynamics in the plant–soil system display non-linear responses to increasing drought intensity both during and after drought, which has implications for plant community recovery trajectories.

KEYWORDS
^{13}C pulse labelling, carbon allocation, drought intensity gradient, drought recovery, drought resistance, grasslands, resource acquisition strategy

1 | INTRODUCTION

The increasing frequency and intensity of extreme weather events, such as drought, heat waves, and floods, threatens ecosystems (IPCC, 2021). The consequences for ecosystem functioning are difficult to predict, as ecological responses to extreme stress are often non-linear (Reichstein et al., 2013; Sippel et al., 2018) and can involve thresholds, defined as an abrupt shift in the state of an ecosystem (Groffman et al., 2006; Hillebrand et al., 2020; Turner et al., 2020). Although thresholds are likely key to understanding the ecological consequences of drought, few studies have explicitly addressed them. This could be due in part to the significant challenges involved in empirically detecting threshold responses (Hillebrand et al., 2020). Recently, thresholds were detected in the response trajectories of individual grassland plant species to drought: abrupt decreases in drought resistance were related with non-linear post-drought overcompensation responses (Ingrisch et al., 2023). Increasing drought intensity could shift plant–soil carbon (C) and nitrogen (N) dynamics, which could alter the plant community's ability to recover after drought (Karlowsky, Augusti, Ingrisch, Hasibeder, et al., 2018). Currently, productivity response to increasing drought intensity in mixed species plant communities is not well understood, and data on shifts in plant–soil C and N dynamics with increasing drought intensity are scarce.

A plant's position on the fast–slow resource economic spectrum has been suggested to inform plant drought response (Grime & Mackey, 2002; Volaire, 2018) and likely shapes how grassland communities respond to increasing drought intensity. The fast–slow resource economic spectrum is a well-defined framework that connects suites of functional traits to define a plant's growth and survival strategy (Grime, 1977; Reich, 2014). Slow-growing/conservative plants that invest in durable tissues better resist drought (Blumenthal et al., 2020; Ingrisch et al., 2018; Karlowsky, Augusti, Ingrisch, Hasibeder, et al., 2018; Pérez-Ramos et al., 2013), while fast-growing/acquisitive plants with N-rich tissues can regrow faster after drought stress has passed (Grime et al., 2000; Karlowsky, Augusti, Ingrisch, Hasibeder, et al., 2018; Lepš et al., 1982; Wilcox et al., 2021). Lesser known is how a plant community's resource acquisition strategy affects productivity thresholds with increasing drought intensity during drought, and productivity recovery afterwards. Abrupt decreases in plant productivity during drought are likely to already occur under mild drought intensities for fast-strategy plant communities as they prioritize growth over durability (Oliveira et al., 2021). Fast-strategy plants are also generally established in environments that are less water and nutrient limited compared to their slow-strategy counterparts (Padullés Cubino et al., 2022; Pérez-Ramos et al., 2012).

A plant community's resource acquisition strategy has been shown to affect plant–soil C cycling (Freschet et al., 2012) and N cycling (Abalos et al., 2019; Grassein et al., 2015; Legay et al., 2014). Drought can modify plant–soil C and N cycling (Chomel et al., 2019; Fuchslueger et al., 2014; Karlowsky, Augusti, Ingrisch, Hasibeder, et al., 2018) by decoupling plant–microorganism interactions (Karlowsky, Augusti, Ingrisch, Akanda, et al., 2018; Rudgers et al., 2020). This disconnect has been attributed to shifts in rhizodeposition, which are known to differ between fast- and slow-strategy plants (Williams & de Vries, 2020). A key outstanding question, however, is whether decoupling of plant–microorganism interactions occurs at different drought intensities for fast- versus slow-strategy plant communities, and whether this has implications for plant community drought resistance and recovery. Under ambient conditions, fast-strategy plants take up more C (CO_2) and have higher rhizodeposition than slow-strategy plants (Henneron, Fontaine, et al., 2020; Henneron, Kardol, et al., 2020), leading to accelerated N cycling in the rhizosphere and higher plant N uptake compared (Kaštovská et al., 2015). Moreover, during drought, plant communities dominated by slow-strategy plant species have been found to allocate more C to root storage and less to soil respiration than communities dominated by fast-strategy plants (Ingrisch et al., 2020; Karlowsky, Augusti, Ingrisch, Hasibeder, et al., 2018). Post-drought, plant communities dominated by fast-strategy plants recover quicker due to a higher capacity for N uptake (Ingrisch et al., 2018; Karlowsky, Augusti, Ingrisch, Hasibeder, et al., 2018). The reported shifts in C allocation during and after drought (Hartmann et al., 2020) determine which functions can be prioritized, for example, storing C in roots for re-growth (Ingrisch et al., 2020; Karlowsky, Augusti, Ingrisch, Hasibeder, et al., 2018), exuding it in the rhizosphere to maintain resource acquisition (Henneron, Fontaine, et al., 2020; Henneron, Kardol, et al., 2020), or allocating to mycorrhizal partners (Sanaullah et al., 2012). Although drought intensity likely influences plant–soil C and N dynamics during drought and recovery, these relationships are not well known.

Here, we determined how two experimental grassland plant communities with contrasting resource acquisition strategies (i.e. fast/acquisitive vs. slow/conservative strategy), respond to increasing drought intensity. In an outdoor mesocosm experiment, we used a ^{13}C pulse-labelling approach to track freshly assimilated C from plants to soil and the microbial community at peak drought and during recovery. Threshold regression modelling was used to identify drought intensity thresholds in plant productivity at peak drought and during recovery. We explored shifts in plant–soil C and N dynamics below and above these productivity thresholds and tested how these dynamics differed between plant communities with contrasting strategies at peak drought and during recovery. We hypothesized that (1) there are thresholds in plant community productivity in response to increasing drought intensity, with the fast-strategy community being less resistant than the slow strategy community; (2) thresholds in post-drought plant productivity overcompensation coincide with thresholds in peak-drought plant productivity, occurring at a lower drought intensity for the fast- than the slow-strategy plant community; (3) increasing drought intensity at peak drought causes an abrupt shift in plant and soil C allocation, with the fast-strategy community increasing C allocation to soil microorganisms and the slow community retaining more C in roots; and (4) increasing drought intensity shifts plant–soil N dynamics after re-wetting, resulting in the fast-strategy community acquiring more N soon after re-wetting than the slow-strategy community.

2 | MATERIALS AND METHODS

2.1 | Experimental setup

An outdoor mesocosm experiment was established at the Botanical Garden, University of Innsbruck, Austria (47°16′04.1″N 11°22′46.3″E), which included five sets of mesocosms (7 L plastic pots, 21 cm Ø, 25 cm height, $n = 210$). Two sets were destructively harvested throughout the experiment at peak drought (set 1), early recovery (set 2), and the final three sets were used for non-destructive measurements throughout the experiment and to monitor recovery (sets 3–5), Figure S1. The drought treatment followed a gradient design, which optimizes the use of experimental units to determine thresholds and non-linear responses (Kreyling et al., 2018). We created the drought intensity gradient by determining the soil water content (SWC, $g_{water}\ g_{fresh\ soil}^{-1}$) at field capacity and then established a gradient of increasing drought intensity (increasing soil water deficit compared to field capacity, SWD) ranging from well-watered controls (20% SWD) to no water added in the drought period (98% SWD). This corresponded with a realized SWD of 18% to 95% (Figure S2B) and a realized SWC of 0.266–0.020 ($g_{water}\ g_{fresh\ soil}^{-1}$). The drought took place 21 July to 12–15 August 2020, when a rainout-shelter was installed over all mesocosms (2.5 m aluminium frame covered with light and UV-B permeable plastic, Lumisol clear AF; Folitec). The drought intensity treatment (SWD) was maintained by weighing and watering the mesocosms 5–7 times per week (Figure S2A). The drought ended when mesocosms were re-wetted to their control weight (20% SWD) over 3 days.

2.2 | Plants and soil

Perennial plant species common to European mesotrophic grasslands were selected based on their traits related to the resource economic spectrum and assembled to create two model grassland plant communities with contrasting strategies: a fast-strategy community (high specific leaf area and leaf N content and low leaf dry matter content) and slow-strategy community (opposite trait values) (Reich, 2014). The fast-strategy community included the grasses *Dactylis glomerata*, *Lolium perenne* and *Phleum pratense*, and the forbs *Leontodon hispidus*, *Plantago lanceolata* and *Rumex acetosa*. The slow-strategy plant community included the grasses *Anthoxanthum odoratum*, *Briza media* and *Festuca rubra* and the forbs *Campanula rotundifolia*, *Leucanthemum vulgare* and *Prunella vulgaris*. Species were selected based on a priori trait values reported in Baxendale et al. (2014), De Long et al. (2019), and de Vries and Bardgett (2016). For confirmation, we measured species-specific leaf dry matter content, specific leaf area and leaf N content of the control communities ($n = 4$) at the peak drought sampling campaign according to Pérez-Harguindeguy et al. (2016). The trait values are reported in Table S1.

Seeds were sourced commercially (*D. glomerata*, *F. rubra*, *L. perenne* and *P. pratense* from Barenbrug BV, the Netherlands; *B. media* and *L. hispidus* from Cruydt Hoek, the Netherlands, and *A. odoratum*, *C. rotondofolia*, *L. vulgare*, *P. lanceolata*, *P. vulgaris* and *R. acetosa* from Jelitto, Germany). Seeds were surface sterilized (1:1 household bleach: tap water for 20 min, then rinsed with tap water), germinated in the same soil used in the experiment, grown for 2 weeks, and then transplanted.

Soil for the experiment was provided from the Botanical Garden, University of Innsbruck. Background soil physiochemical factors of the bulk soil were determined (see Supplementary Methods). The soil was a sandy loam: 53.5% sand (50–2000 µm), 35.6% silt (2–50 µm) and 10.8% clay (<2.0 µm). Initial chemical properties were as follows: 0.29% total N, 1.1 g kg^{-1} plant available P, 3.575 plant available g kg^{-1} K, 6.12% total C (i.e. organic and inorganic C), 7.57% organic matter (loss on ignition method) and a pH_{CaCl2} of 7.67. The soil was sieved to 1 cm, mesocosms were filled with fresh soil (5.76 kg dw equivalent), moistened to a 20% SWD (0.248 $g_{water}\ g_{fresh\ soil}^{-1}$) and the weight was recorded. Two seedlings per plant species (12 individuals pot^{-1}, 346 individuals m^{-2}) were transplanted 27 May–1 June 2020. Dead seedlings were replaced over 10 days. Mesocosms were maintained at 20% SWD until the drought and fertilized (20 kg N ha^{-1} as urea) on 22 June 2020. Climatic conditions are reported from a nearby climate station (TAWES UIBK), provided by the Austrian Weather Service ZAMG (https://www.zamg.ac.at/) and the Department of Atmospheric and Cryospheric Sciences, University of Innsbruck (Figure S3A).

2.3 | Plant biomass

Species-specific above-ground biomass was harvested 1 week before the drought started, at peak drought, and *c.* 2 months after re-wetting. Above-ground biomass was cut to 3 cm above the soil surface, dried at 60°C for 72 h and weighed. Below-ground biomass was determined at peak drought and early recovery (12 days after re-wetting) by washing soil from roots over a 0.5 mm sieve. Clean roots were dried at 60°C for 72 h and weighed.

2.4 | Non-destructive monitoring

We measured net ecosystem exchange (NEE), ecosystem respiration (ER), normalized difference vegetative index (NDVI) and canopy height 18 times throughout the experiment. Measurements began on 20 July 2020, and continued through to 9 October 2020. Gross primary productivity (GPP_{sat}) was estimated with the paired measurements of NEE and ER (see Supplementary Methods).

2.5 | Leaf and root N

Community leaf N concentration was determined by harvesting the youngest, fully expanded leaf of each plant species at peak drought and 12 days after re-wetting, followed by drying at 60°C for 72 h. At peak drought, leaves were pooled per mesocosm based on the species-specific relative abundance of their above-ground biomass. Twelve days after re-wetting, leaf N concentration was determined at the species level and then the community-weighted mean was calculated. Samples were ground to a fine powder using a Tissue Lyser II (Qiagen), weighed into tin cups (art.no. 176.9811.26; IVA Analysetechnik GmbH & Co.KG) and analysed with a Flash EA1112 elemental analyser (Thermo Electron Corporation). Community root N concentration was determined in the same way. Peak drought whole plant N pool (g N m^{-2} ground area) was calculated as N concentration in above-ground biomass (leaves, given the very minor fraction of stems present in the mesocosms) and below-ground biomass (roots) multiplied by above-ground/below-ground biomass harvested at peak drought. Whole plant N uptake is the N acquired in the 12 days following re-wetting (i.e. the sum of above-ground and below-ground N pools at early recovery minus the belowground N pool at peak drought).

2.6 | Soil N and pH

Ammonium (NH_4^+-N) and nitrate (NO_3^--N) were determined according to Schinner et al. (1996) by shaking 7.5 g fresh soil in 30 mL 0.0125 M $CaCl_2$ for 1 h at 170 rpm, filtering (Macherey & Nagel 615¼, 150 mm filter paper) and analysing on a spectrophotometer (Hitachi U-2001) at 660 nm and 210 nm, respectively. Dissolved N was quantified on a TOC-L/TNM-L analyser (Shimadzu Co., Japan) after extracting 7.5 g fresh soil in 30 mL distilled water by shaking for 30 min at 120 rpm.

2.7 | ^{13}C pulse labelling and sampling campaigns

2.7.1 | Pulse labelling

We performed a ^{13}C-pulse-labelling campaign at peak drought (after 21 days of drought) and at early recovery (7 days after re-wetting) in line with Karlowsky, Augusti, Ingrisch, Hasibeder, et al. (2018) and Ingrisch et al. (2020). At each campaign, mesocosms were fit into a custom-built, air-tight frame and chamber. At peak drought fast- and slow-strategy communities were pulse labelled on 11 and 12 August 2020, respectively. At early recovery, all plant communities were pulse labelled on 20 August 2020. Microclimatic conditions were similar on all 3 days (Figure S3B). Inside the chamber, air was ventilated with fans and temperature regulated by circulating ice-cold water through tubes. During labelling, we continuously monitored CO_2 concentration and ^{13}C isotope ratio (G2101i Analyzer; Picarro Inc., USA), air temperature and humidity (HMP 75; Vaisala, Finland), and photosynthetically active radiation, PAR (PQS, Kipp & Zonen, Germany). Labelling took place for 90 min between 10 am and 1 pm, beginning when PAR reached 1500 µmol m^{-2} s^{-1}. When CO_2 dropped to 250 ppm, pulses of highly enriched $^{13}CO_2$ (99.00 atom-% ^{13}C, Sigma-Aldrich) were added with a syringe to maintain approximately 50 atom-% ^{13}C and 500–600 ppm CO_2 (Table S2).

2.7.2 | Sampling

Natural abundance $\delta^{13}C$ in leaves, roots, microbial biomass C, extractable organic C (EOC), and phospholipid fatty acid (PLFA) and neutral lipid fatty acid (NLFA) were determined the day prior to labelling on a separate set of mesocosms. Leaves were harvested at the species level, immediately treated by microwave to stop metabolic activity, and dried at 60°C for 72 h. Two soil cores per pot (2 cm Ø, 25 cm depth) were taken with a core, pooled and sieved to 2 mm. Soil was divided and stored at 4°C for microbial biomass C or at −80°C for PLFA and NLFA analyses. Roots that remained on the sieve were washed, treated by microwave and dried at 60°C for 72 h.

After pulse labelling, we sampled shortly after the chamber was opened (*c.* 15 min for leaves, 20–120 min for soil and 25–140 min for roots), after 48 h, and after 120 h. Each sampling campaign was carried out in the same way as the natural abundance $\delta^{13}C$ sampling.

2.8 | Plant leaf and root isotopic C composition

The $\delta^{13}C$ of leaves and roots was determined by grinding dried biomass into a fine powder, weighing into tin cups (art.no. 176.9811.26;

IVA Analysetechnik GmbH & Co.KG) and measuring total C and $\delta^{13}C$ with elemental analysis (EA)—isotope ratio mass spectrometry (IRMS; EA 1100, CE Elantech; coupled to a Delta+ IRMS; Finnigan MAT). Leaves were pooled per community based on the relative abundance of species-specific leaf biomass and capsulized the tin cups.

2.9 | NLFA and PLFA content and C isotopic composition

We characterized the uptake of recent plant-derived C into broad microbial groups by determining ^{13}C incorporation into PLFAs and NLFAs, which were extracted from frozen soil according to Bligh and Dyer (1959) and Karlowsky, Augusti, Ingrisch, Akanda, et al. (2018) (see Supplementary Methods). Briefly, fatty acid methyl esters (FAMEs) were quantified by gas chromatography–flame ionization detection. Compounds were identified and biomass was derived from peak area using a standard curve with increasing concentrations of a mixture of known FAMEs (Supelco 37 Component FAME Mix; Sigma-Aldrich Chemie GmbH; BR2 and BR4 mixture, Larodan Fine Chemicals AB). FAME ^{13}C isotope content was corrected for the methyl group introduced during derivatisation, and for offset and drift. We used the sum of PLFA markers i14:0, i15:0, a15:0, i16:0, a17:0, i17:0 and br18:0 for Gram-positive bacteria (Zelles, 1999), 10Me16:0 and 10Me18:0 for Gram-positive actinobacteria (Lechevalier et al., 1977), 16:1ω7 and 18:1ω7 for Gram-negative bacteria (Zelles, 1997, 1999), 18:2ω6,9c for saprotrophic fungi (Frostegård & Bååth, 1996), and the NLFA 16:1ω5 as a marker for arbuscular mycorrhizal fungi (AMF) (Mellado-Vázquez et al., 2016; Olsson, 1999). Total fungal abundance was calculated using the NLFA 16:1ω5 and PLFAs 16:1ω5, 18:2ω6,9c. Total bacteria included all markers representing bacteria (above) plus 14:0 and 15:0 (Canarini et al., 2021).

2.10 | C isotopic composition of soil-EOC and microbial biomass carbon

EOC and microbial biomass C were determined using chloroform fumigation method (Voroney et al., 2007), see Supplementary Methods. Microbial biomass C was calculated as:

$$\text{Microbial biomass C} = (\text{EOC fumigated} - \text{EOC nonfumigated}) / 0.45,$$

where 0.45 is the extraction efficiency of microbial biomass C after chloroform fumigation (Vance et al., 1987). The $\delta^{13}C$ signatures of EOC were determined after Scheibe et al. (2012): 900 µL extract was acidified with 35 µL 10% HCl, flushed with N_2 for 15 min and analysed in triplicate with HPLC-IRMS (Dionex UltiMate 3000 UHPLC coupled via a LC-IsoLink system to a Delta V Advantage IRMS, Thermo Fisher Scientific).

2.11 | C isotopic composition of soil respiration

Soil respiration and its isotopic composition were continuously measured for 5 days after labelling using a custom-made measurement setup (see Ingrisch et al., 2020), modified to consecutively measure 23 soil respiration chambers with a C isotope analyser (Picarro G2131-i; Picarro Inc.), see Supplementary Methods.

2.12 | Calculation of incorporated ^{13}C

Incorporated ^{13}C was calculated as the total amount of ^{13}C in a plant, soil or microbial C pool in line with Hafner et al. (2012):

$$R_{\text{sample}} = \left(\frac{\delta^{13}\text{C}}{1000} \times R_{\text{VPDB}}\right) + R_{\text{VPDB}}, \quad (1)$$

$$\chi\left(^{13}\text{C}\right)_{\text{sample}} = \left(\frac{R\text{sample}}{R\text{sample} + 1}\right), \quad (2)$$

$$\chi E\left(^{13}\text{C}\right) = \chi\left(^{13}\text{C}\right)_{\text{sample}} - \chi\left(^{13}\text{C}\right)_{\text{natural abundance}}, \quad (3)$$

$$\text{Incorporated } 13\text{C}_t = \chi E\left(^{13}\text{C}\right) \times \text{Cpool}, \quad (4)$$

$$\chi\left(^{13}\text{C}\right)_{\text{microbial biomass C}} = \frac{\chi\left(^{13}\text{C}\right)_{\text{TOC}} \times \text{TOC} - \chi\left(^{13}\text{C}\right)_{\text{EOC}} \times \text{EOC}}{(\text{TOC} - \text{EOC})}, \quad (5)$$

where (1) R_{VPDB}=0.011180, the $^{13}C/^{12}C$ ratio in Vienna Pee Dee Belemnite, (2) $\chi\left(^{13}\text{C}\right)_{\text{sample}}$ is the ^{13}C atom fraction, (3) $\chi\left(^{13}\text{C}\right)_{\text{microbial biomass C}}$ is calculated according to the isotopic mass balance (4) $\chi E\left(^{13}\text{C}\right)$ is the ^{13}C enrichment in a C pool, derived from subtracting the atom fraction of ^{13}C in the natural abundance sample from fraction of ^{13}C in the enriched sample, and (5) incorporated $^{13}C_t$ is the excess atom fraction of ^{13}C multiplied by the respective C pool at a given time (*t*).

Soil respiration rate (µmol m^{-2} s^{-1}) was calculated as:

$$\text{SR} = \frac{f \times (\text{CO}_{2\,\text{out}} - \text{CO}_{2\,\text{in}})}{A}, \quad (6)$$

where *f* is the flow rate through the chamber, CO_{2out} and CO_{2in} are the mean concentrations at the chamber outlet and in the buffer volume, respectively, and *A* the area of the chamber (m^2).

The isotopic composition of soil respiration $\chi(^{13}C)_{SR}$:

$$\chi\left(^{13}\text{C}\right)_{\text{SR}} = \frac{\chi\left(^{13}\text{C}\right)\text{out} \times \text{CO}_{2\,\text{out}} - \chi\left(^{13}\text{C}\right)\text{in} \times \text{CO}_{2\,\text{in}}}{\text{CO}_{2\,\text{out}} - \text{CO}_{2\,\text{in}}}, \quad (7)$$

where $\chi(^{13}C)_{in}$ and $\chi(^{13}C)_{out}$ denote the atom fraction of $^{13}CO_2$ in the buffer volume and the chamber outlet, respectively, which were calculated from the mean concentrations of the two isotopologues $^{12}CO_2$ and $^{13}CO_2$.

The absolute rate of ^{13}C label efflux in soil respiration (mg ^{13}C m^{-2} h^{-1}) is calculated as:

$$\text{incorporated}^{13}C_{SR} = \chi E\left(^{13}C\right)_{SR} \times SR. \quad (8)$$

The cumulative amount of respired ^{13}C label was calculated for each mesocosm according to the trapezoid rule (linear interpolation between consecutive measurements).

Relative partitioning of ^{13}C was calculated by dividing the incorporated ^{13}C in one compartment and time point by the total ^{13}C measured in all compartments at *T*0.

2.13 | Data analysis

Statistical analyses were performed in R version 4.1.0 (R Core Team, 2020). Figures were made using GGPLOT (Wickham, 2016), COWPLOT (Wilke, 2019) and PATCHWORK (Pedersen, 2020). Productivity thresholds were identified using threshold regression models using the R-package CHNGPT (Fong et al., 2017). We considered two types of threshold responses: (i) continuous thresholds that change the relationship of productivity with SWD and (ii) discontinuous thresholds that cause abrupt changes in the value of productivity (Berdugo et al., 2020; Groffman et al., 2006). Continuous thresholds were modelled by segmented regressions (change in the model slope at a threshold) and discontinuous thresholds by step regressions (change in model intercept at a threshold). Threshold models were only considered if Akaike information criterion (AIC) was smaller than corresponding linear and quadratic regressions. Thus, the presented threshold models have superior data fit than do linear or quadratic regressions. Threshold estimations for the best model type were repeated with 1000 bootstrapped samples to estimate the distribution of each threshold.

To determine the effect of drought intensity and plant community on all dependent variables, we tested the effect of SWD (continuous), plant community (ordered factor) and their interaction using generalized additive models (GAMs) with the function gam from the R-package MCGV (Wood, 2011). GAMs allow for linear and non-linear relationships, reported in the edf statistic, where 1.0 is a linear relationship. We modelled the following relation:

$$Y = \beta_0 + \beta_1(\text{plant community}) + \beta_1(\text{SWD}) + f_1(\text{SWD, plant community}),$$

where β_0 represents the intercept, $\beta_{1(\text{plant community})}$ the effect of the plant community (fast- or slow-strategy), $\beta_{1(\text{SWD})}$ the overall effect of SWD and $f_1(\text{SWD, plant community})$ the interactive effect between SWD and plant community. When a significant interaction was detected, we determined the effect of SWD within each plant community by modelling the relation (where plant community is considered a factor: fast or slow strategy):

$$Y = \beta_0 + \beta_1(\text{plant community}) + f_1(\text{SWD, plant community}).$$

Model fit was checked using gam.check from the R-package MCGV (Wood, 2011). Models with different smoothers and families were compared using AIC and the best fit model (lowest AIC) was retained. We tested how SWD affected overall ^{13}C incorporation into PLFAs and NLFA of interest using principle component analysis (PCA) with the function pca from the R-package FACTOMINER (Le et al., 2008) on scaled (mean 0, sd ± 1) data.

3 | RESULTS

3.1 | Drought intensity effects on plant productivity

Increasing drought intensity decreased above-ground biomass at peak drought and increased above-ground biomass 2 months post-drought in both plant communities with distinct thresholds (Figure 1a,b). The threshold responses were best described by step-regression models, which reflect an abrupt shift in the relationship between above-ground biomass and drought intensity. At peak drought, thresholds were detected at 65% SWD for the fast-strategy community and 75% SWD for the slow-strategy community, where

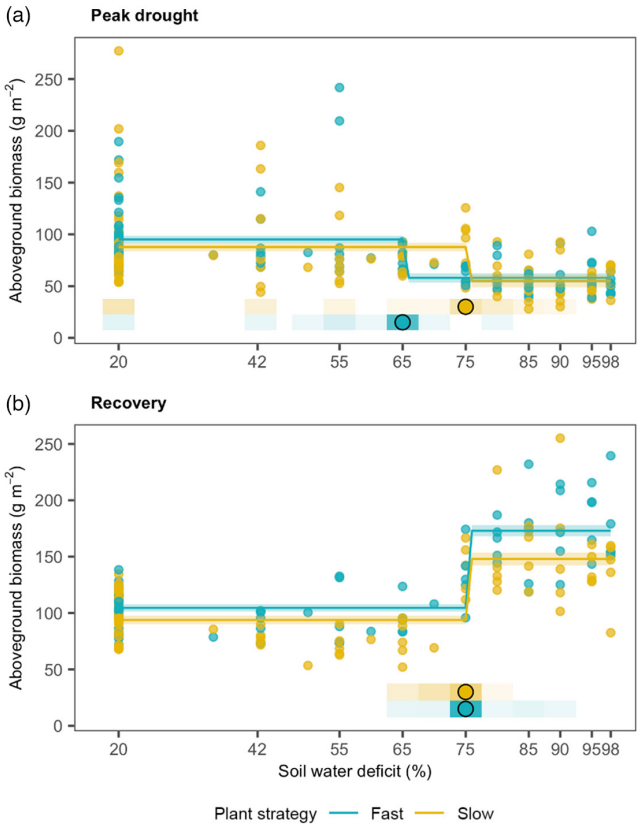

FIGURE 1 Drought intensity (expressed as soil water deficit, %) effects on plant community above-ground biomass (living and senesced plant tissues) at (a) peak drought (after a 3-week drought) and (b) recovery (*c*. 2 months after re-wetting) for the fast- and slow-strategy community. Points indicate individual mesocosms and lines denote the best-fit thresholds regression models and their 95% confidence intervals. Colour density of the shaded boxes indicates the bootstrapped distribution of threshold estimates with the best-fit threshold indicated by the point.

above-ground biomass sharply decreased by 37.3% and 31.4%, respectively. During the 3-week drought, there were no significant interaction effects between drought intensity and plant community strategy on GPP, NDVI or canopy height (Figures S4–S6; Tables S6–S8). Thus, the slow community was more drought resistant than the fast-strategy community, in terms of above-ground biomass, but this did not translate into other measures of productivity.

Two months after re-wetting, a threshold at 75% SWD increased above-ground biomass by 38.6% and 39.2% for the fast- and slow-strategy community, respectively (Figure 1b). Considering all communities that experienced a drought intensity above the threshold detected at 75% SWD (Figure 1b), the fast-strategy community produced significantly more above-ground biomass than the slow-strategy community ($F_{1,58}=4.95$, $p<0.05$). After re-wetting, the recovery responses of the fast- and the slow-strategy community diverged, and overshoot in GPP and canopy height began sooner for the fast- than the slow-strategy community (Figures S4 and S6), while NDVI recovery responses were similar (Figure S5).

3.2 | Plant/soil carbon dynamics

At peak drought, both plant communities responded similarly to increasing drought intensity, which decreased C uptake and incorporation into roots, EOC and microbial biomass C in soil (Figure 2; Table S3). Increasing drought intensity increased the relative amount of ^{13}C partitioned to leaves and microbial biomass, while ^{13}C partitioned to roots decreased (Figure S7; Table S9). Overall, the fast-strategy community partitioned more ^{13}C to roots than the slow community (Figures S7D). In both plant communities, increasing drought intensity decreased ^{13}C incorporation into PLFA and NLFAs, with the exception of PLFAs representing actinobacteria which increased (Figure 3; Table S5). ^{13}C incorporation into PLFAs/NLFA in communities that experienced a drought above the productivity threshold (identified in Figure 1) were separated from those that experienced a milder drought or control (Figure S11A).

Recovery trajectories differed between fast- and slow-strategy communities. Seven days after re-wetting, ^{13}C incorporation in leaves and roots of the slow-strategy community significantly decreased with increasing past drought intensity, while the fast-strategy community was no longer affected (Figure 2b,d). In both plant communities, past drought intensity increased ^{13}C incorporated into extractable organic and microbial biomass C. Soil respired ^{13}C (cumulative over 5 days) decreased with increasing past drought intensity in both communities (Figure 2f,h,j). In the slow community only, increasing past drought intensity increased the relative partitioning of ^{13}C to microbial biomass and decreased ^{13}C partitioned to leaves (Figure S8). After re-wetting, the soil water deficit during the drought significantly affected ^{13}C incorporation into fatty acids (Figure 3). Past drought intensity increased ^{13}C incorporation into PLFAs representing actinobacteria in both plant communities (Figure 3b) and increased ^{13}C incorporated into PLFAs representing Gram-positive bacteria in the fast community only (Figure 3f). ^{13}C incorporation into the NLFA representing AMF decreased with past drought intensity (Figure 3h), while ^{13}C incorporation into PLFA and NLFAs representing Gram-negative bacteria or saprotrophic fungi were no longer affected (Figure 3d,j). The ^{13}C incorporated into the PLFAs/NLFA in communities that experienced a drought above the productivity threshold (identified in Figure 1) were grouped and separated from those that experienced a milder drought or control (Figure S11B).

3.3 | Plant/soil N dynamics

At peak drought, increasing drought intensity affected soil N dynamics similarly for both plant communities. Soil NO_3^--N was non-linearly related to increasing drought intensity, first decreasing and then increasing at the highest drought intensities (Figure S9A). Soil NH_4^+-N and dissolved N increased with increasing drought intensity in both communities (Figure S9B,C). At peak drought, leaf N concentration was not affected by drought intensity (Figure 4a; Table S4), while fast community root N concentration increased with increasing drought intensity (Figure 4c). Whole plant N pool ($g\,N\,m^{-2}$ ground area) decreased for both plant communities with increasing drought intensity (Figure S10A; Table S4).

Twelve days after re-wetting, we found that past drought intensity increased NO_3^--N and dissolved N in both communities, while soil NH_4^+-N was not affected (Figure S9D–F). Leaf N concentration increased with past drought intensity in both communities (Figure 4b), and drought intensity no longer affected root N concentration (Figure 4d). Whole plant N uptake ($g\,N\,m^{-2}$ ground area) increased with increasing past drought intensity for the fast-strategy community only. The slow-strategy plant community's whole plant N uptake was not affected by increasing past drought intensity (Figure S10C).

4 | DISCUSSION

4.1 | Drought intensity thresholds of productivity

Thresholds in grassland response to increasing drought intensity are poorly understood, despite playing a key role in informing ecosystem functioning during and after drought (Grünzweig et al., 2022; Turner et al., 2020). Using model grassland communities established in outdoor mesocosms, we identified distinct thresholds in plant community productivity in response to increasing drought intensity during drought and recovery. We found that abrupt decreases in plant community productivity during drought were coupled to productivity overcompensation during recovery, as previously demonstrated for monocultures of two grassland plant species (Ingrisch et al., 2023). Thus, drought intensity plays an important role in determining plant community drought response both during drought and after re-wetting (see Figure 5 for an overview of our findings).

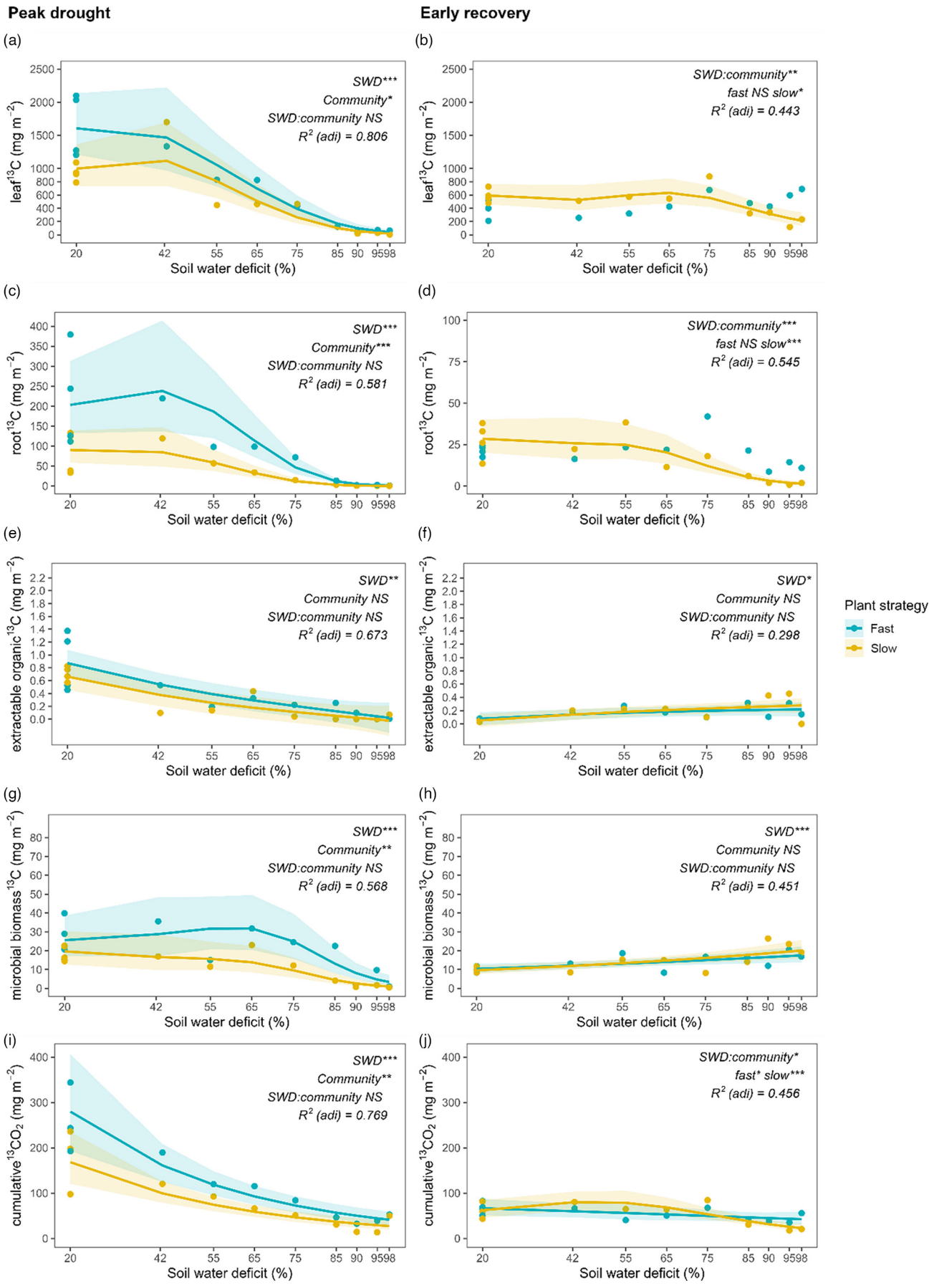

FIGURE 2 Incorporated ^{13}C in (a) leaves directly after labelling at peak drought and (b) at early recovery, and 5 days after pulse labelling in (c, d) roots, (e, f) microbial biomass C, (g, h) extractable organic C and (i, j) cumulative soil-respired $^{13}CO_2$. Lines indicate the best fit generalized additive model (GAM), and shaded area around the line depicts the model-predicted 95% confidence interval. Significance is noted between the plant communities (Community), over the drought gradient (SWD) and the interaction (SWD: community). Within community significance is shown with a significant interaction (fast, slow). $p < 0.001^{***}$, $p < 0.001^{**}$, $p < 0.05$. R^2 adjusted indicates the explained variation of the GAMs (Table S4).

Confirming our first hypothesis, the threshold in plant community productivity at peak drought occurred at a lower drought intensity for the fast- than the slow-strategy community (Figure 1). This indicates that the fast-strategy community was less drought resistant than the slow-strategy community, broadly consistent with earlier studies which considered one level of drought intensity (Ingrisch et al., 2018; Karlowsky, Augusti, Ingrisch, Hasibeder, et al., 2018; Pérez-Ramos et al., 2013). Fast-growing plant species are more vulnerable to drought stress because of the trade-off between traits that enable fast resource acquisition and those that facilitate hydraulic safety, for example, leaf density and osmotic potential (Díaz et al., 2016; Reich, 2014; Wilcox et al., 2021). In contrast, slow-growing plant species have a stress-tolerating strategy (Grime & Mackey, 2002) that allows them to reduce water use, avoid turgor loss and maintain lower levels of growth throughout the drought, conferring higher resistance (Pérez-Ramos et al., 2013).

After the drought ended, the fast-strategy community had greater capacity for recovery, confirming our second hypothesis. Post-drought, the fast-strategy community recovered quicker than the slow-strategy community in terms of GPP, and 2 months after re-wetting had significantly more above-ground biomass (i.e. compensatory growth) above the productivity threshold. The quicker recovery of the fast-strategy community supports our second hypothesis and previous studies that fast-strategy communities have greater capacity to recover from drought, despite having lower resistance than slow-strategy communities (Ingrisch et al., 2018; Karlowsky, Augusti, Ingrisch, Hasibeder, et al., 2018). The overshoot in GPP was maintained until the end of the experiment and is consistent with the overshoot in above-ground biomass found 2 months after re-wetting (Figure 1b). Our results demonstrate that increasing drought intensity leads to abrupt shifts in productivity (both above-ground biomass and GPP) at peak drought, which differ between fast- and slow-strategy communities and likely have implications for plant community recovery trajectories.

4.2 | Plant/soil C dynamics

4.2.1 | Peak drought

Previous studies have found that drought reduces C uptake, below-ground C allocation and soil respiration (Chomel et al., 2019, 2022; Fuchslueger et al., 2014; Ingrisch et al., 2020; Karlowsky, Augusti, Ingrisch, Hasibeder, et al., 2018). Our study suggests that the extent to which such reductions occur depends on drought intensity (Figure 2). Considering the relative partitioning of recent plant-assimilated C, we found that drought intensity increased the relative proportion of C partitioned to leaves and transferred to the soil microbial biomass, while decreasing C partitioned to the roots (Figure S7). In previous research, drought effects on the relative partitioning of recent C vary, with studies reporting increases in relative C retention above-ground (Chomel et al., 2019; Sanaullah et al., 2012), increases in below-ground C allocation (Karlowsky, Augusti, Ingrisch, Hasibeder, et al., 2018) or no clear drought effect (Hasibeder et al., 2015). Such discrepancies could be caused by differences in drought intensity, as we show that C partitioning changes with increasing drought intensity (Figure S7).

In contrast to our third hypothesis, shifts in plant–soil C dynamics with increasing drought intensity at peak drought were similar between the fast- and the slow-strategy communities (i.e. there were no interactive effects between plant community and drought intensity, Figure 2). Over the drought gradient, C uptake by the fast-strategy community was higher than for the slow-strategy community, which is in line with previous research (Henneron, Fontaine, et al., 2020; Henneron, Kardol, et al., 2020). However, relative ^{13}C partitioning to the compartments we measured was similar between fast- and slow-strategy plant communities (Figure S7). Previous studies have reported larger drought effects on C-cycling in grasslands dominated by fast- compared to slow-strategy plant species (Ingrisch et al., 2020; Karlowsky, Augusti, Ingrisch, Hasibeder, et al., 2018). However, in these field studies, the effect of species composition, management and edaphic soil characteristics between the grasslands could not be separated. In our controlled outdoor mesocosm experiment, we are able to isolate plant strategy effects on drought responses. Still, considering that plant resource acquisition strategy influences both plant–soil C-cycling (Henneron, Fontaine, et al., 2020; Henneron, Kardol, et al., 2020) and drought resistance (Pérez-Ramos et al., 2013), it is surprising that we did not find differences in the response of C incorporation to drought intensity for the fast- and slow-strategy communities.

In our study, small differences in C incorporation between fast- and slow-strategy communities could be a consequence of studying these perennial communities in their first year of growth. As plant communities with different resource acquisition strategies develop, differences in their plant–soil C dynamics likely increase due to contrasting leaf and root lifespan (Lind et al., 2013) and feedbacks to decomposition processes (Freschet et al., 2012). Differences in the associated microbial communities could also become stronger in subsequent growing seasons because of differences in plant–soil feedbacks between fast- and slow-strategy plants (Baxendale et al., 2014; Spitzer et al., 2021; Xi et al., 2021). While our findings show that increasing drought intensity has an overriding effect on

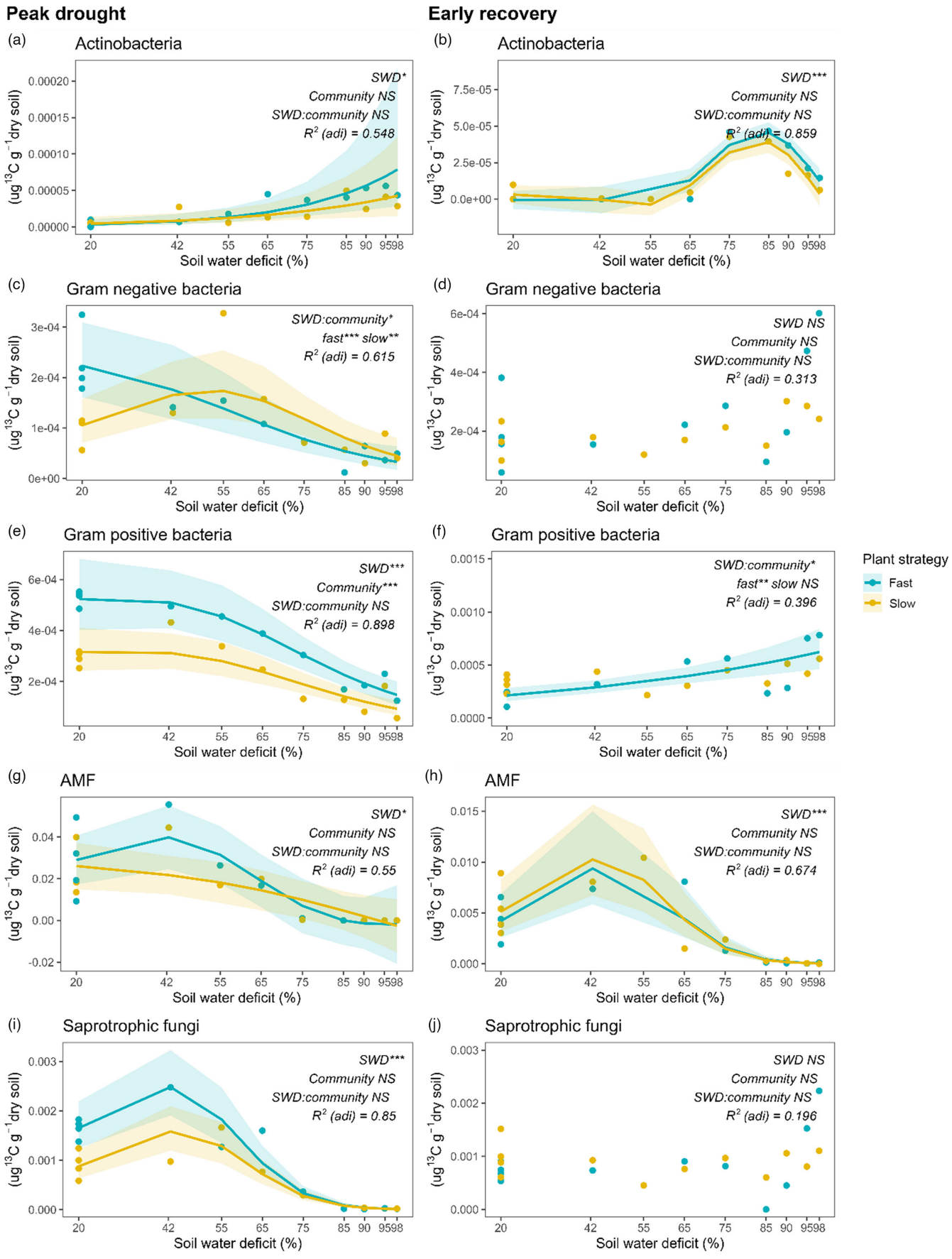

FIGURE 3 Drought intensity (soil water deficit) effects on incorporated ^{13}C at peak drought in phospholipid fatty acids (PLFAs) representing (a) actinobacteria, (c) Gram-negative bacteria, (e) Gram-positive bacteria, and (i) saprotrophic fungi, and (g) the neutral lipid fatty acid (NLFA) representing arbuscular mycorrhizal fungi (AMF), and at early recovery (b, d, f, h, j). For list of PLFA and NLFAs considered, see Section 2. *p* values show the effect of drought intensity (soil water deficit, SWD), plant community (Community), and their interaction on the response variable based on a generalized additive model (GAM). If a significant interaction was found, a second GAM model was used to test the relationship between drought intensity and the response variable within each plant communities. $p < 0.001^{***}$, $p < 0.01^{**}$, $p < 0.05^{*}$. R^2 adjusted indicates the explained variation of the GAM model, for full statistical output, see Table S5.

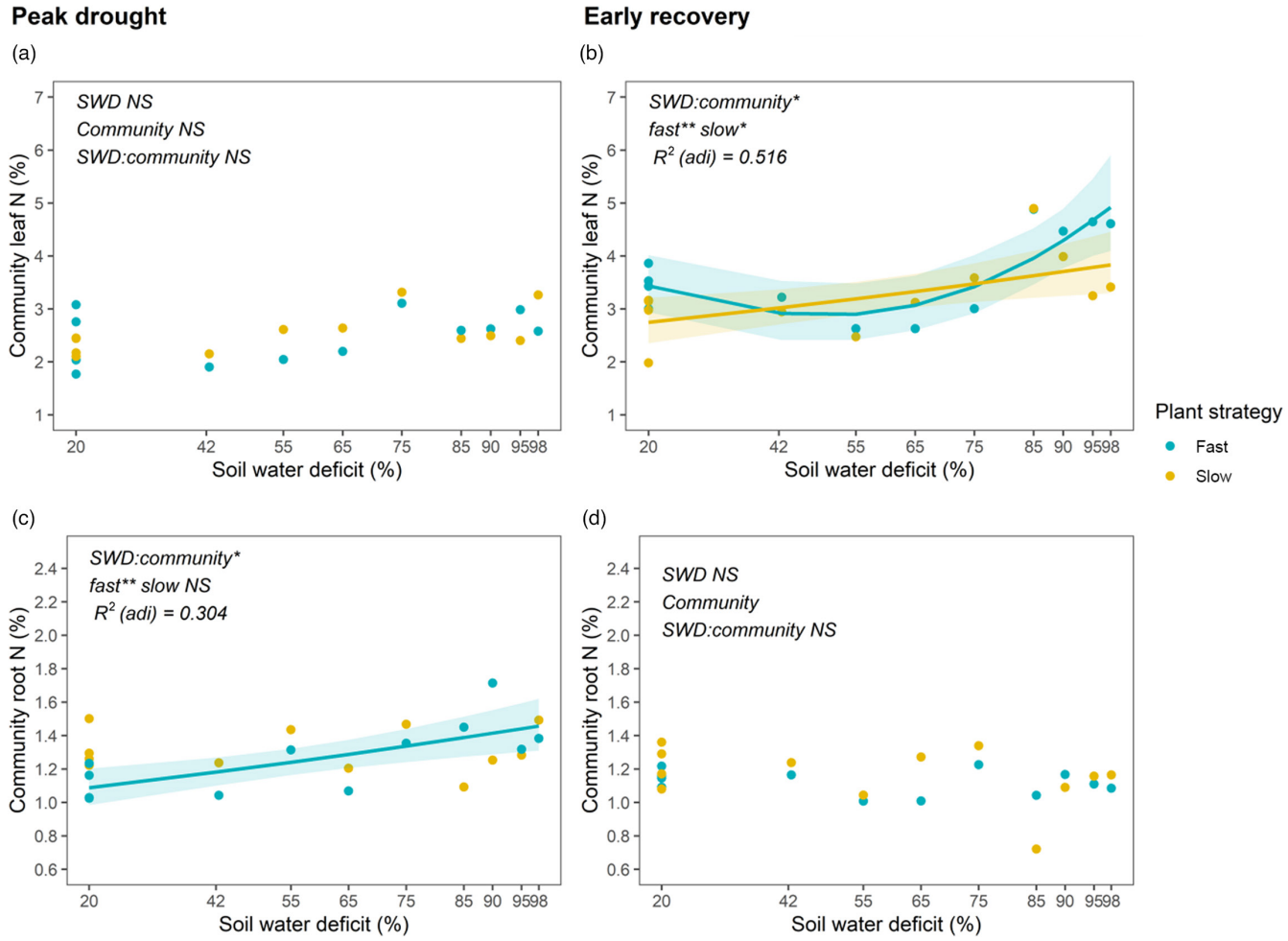

FIGURE 4 Nitrogen (N) concentration in leaves at (a) peak drought and (b) early recovery (the soil water deficit refers to the soil water deficit at peak drought), and in roots at (c) peak drought and (d) early recovery.

plant–soil C allocation at peak drought, we expect that in following growing seasons, plant resource strategies could play a larger role in mediating C dynamics during drought.

Shifts in plant–soil C dynamics could disconnect plants and microorganisms during drought via changes in rhizodeposition (Karlowsky, Augusti, Ingrisch, Akanda, et al., 2018; Williams & de Vries, 2020). In field and glasshouse studies, drought has been reported to weaken the link between plants and the microbial community by reducing C flow from recent photosynthates to below-ground pools (Chomel et al., 2019; Fuchslueger et al., 2014), decreasing C incorporation into microbial biomass (Karlowsky, Augusti, Ingrisch, Akanda, et al., 2018; Karlowsky, Augusti, Ingrisch, Hasibeder, et al., 2018) and mesofauna (Chomel et al., 2019, 2022; Seeber et al., 2012). Our findings support this, as ^{13}C incorporation into PLFAs representing Gram-positive bacteria, Gram-negative bacteria and saprotrophic fungi, as well as the NLFA representing AMF decreased with increasing drought intensity (Figure 3). AMF can play an important role in resource uptake (Pantigoso et al., 2022), reducing drought stress (Wu, 2017) and mitigating decreases in plant productivity (Jia et al., 2020). However, the sharp decrease in ^{13}C incorporation into the NLFA representing AMF could signal that either drought disrupts the plant–AMF connection or that ^{13}C is prioritized elsewhere. Previous studies considering drought effects on ^{13}C incorporation in this NLFA are inconsistent, showing that ^{13}C transfer during drought is maintained (Chomel et al., 2019, 2022; Fuchslueger et al., 2014) or reduced (Karlowsky, Augusti, Ingrisch, Hasibeder, et al., 2018).

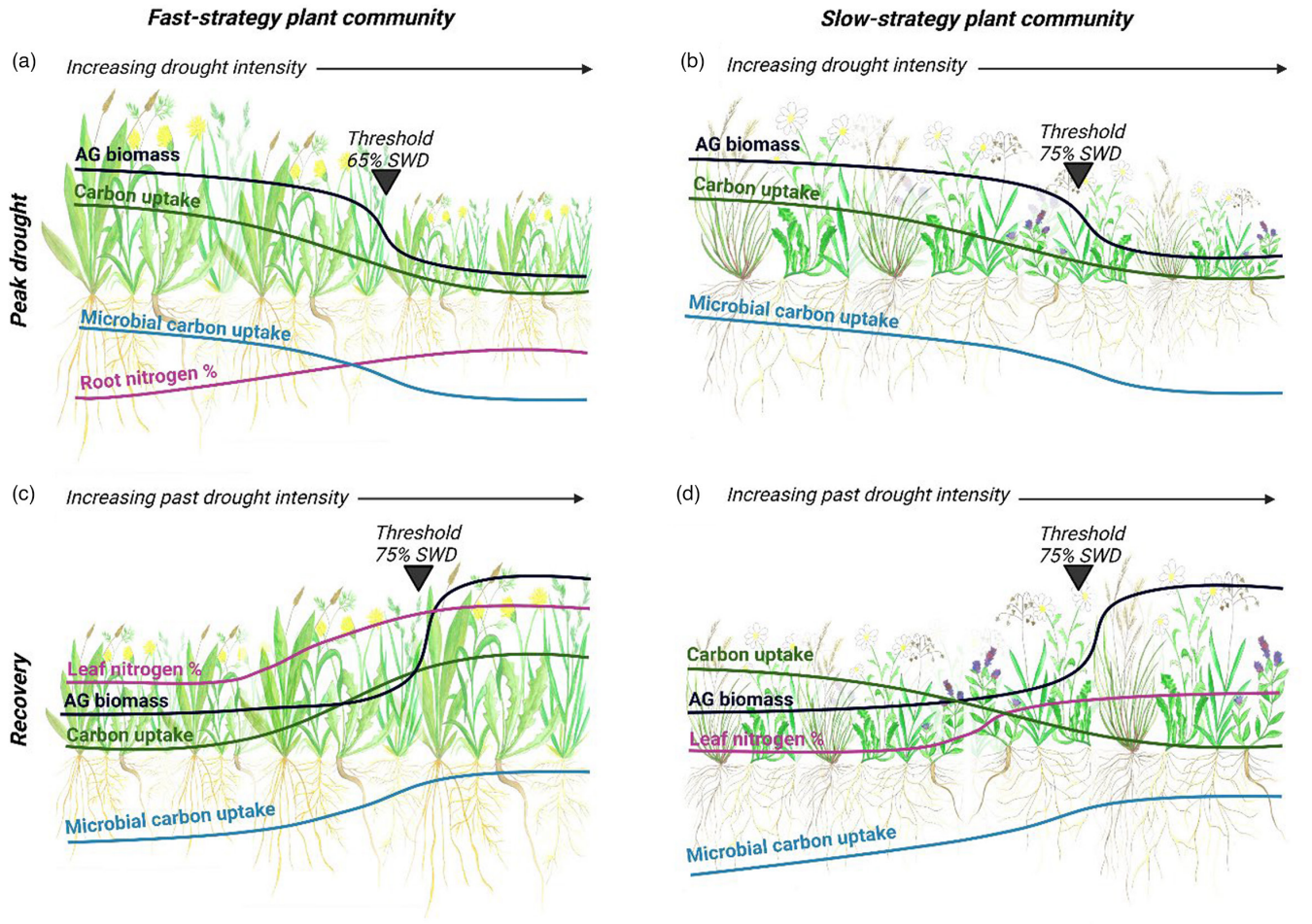

FIGURE 5 Summary of key findings of our major response variables: above-ground (AG) biomass, plant and microbial C uptake and leaf/root N concentration. At peak drought, increasing drought intensity reduced AG biomass, plant C uptake and microbial C uptake in both (a) fast- and (b) slow-strategy plant communities. Root N concentration (%) increased with increasing drought intensity in the fast-strategy community only. The fast-strategy community was less resistant, reaching the productivity threshold at a lower drought intensity (65% soil water deficit, SWD) than (b) the slow-strategy community (75% SWD), indicated by the black triangle. Post-drought, microbial C uptake increased with past increasing drought intensity in both plant communities soon after re-wetting (c, d), signalling a fast microbial recovery. (c) The fast-strategy community recovered quicker, and began overshooting in terms of plant C uptake sooner (i.e. within 10 days of re-wetting) than (d) the slow-strategy community (the 'carbon uptake' lines indicate the C taken up soon after re-wetting). Leaf N concentration (%) in both communities increased with increasing past drought intensity. Two months post-drought, we found thresholds in overshoot in both plant communities (indicated by the black triangle). Lines indicate a significant relationship was found, absence of the line indicate no relationship. Figure made with BioRender, drawings by NJO.

However, our results suggest that drought intensity could be an overlooked driver in plant C transfer to this NLFA, and that directly considering drought intensity may reconcile previously reported discrepancies. We found that at drought intensity between 42% and 65% SWD the amount of ^{13}C allocated to the NLFA representing AMF was similar to the control (20% SWD), while increasing drought intensity to over 75% SWD caused a sharp decrease (Figure 3).

In contrast, the ^{13}C incorporated into actinobacteria PLFAs increased with increasing drought intensity (Figure 3). Actinobacteria are spore forming and able to persist in stressful environments (Taketani et al., 2017). Their ability to tolerate drought (Naylor et al., 2017) may have enabled them to continue functioning as drought intensity increased. An increase in their relative abundance during extreme drought, which has been previously reported (Naylor et al., 2017; Pérez Castro et al., 2019), may have also contributed our finding that ^{13}C incorporation into actinobacteria PLFAs increased with drought intensity.

4.2.2 | Recovery

One week after re-wetting, C uptake by the fast-strategy community was no longer affected by drought intensity (Figure 2), signalling its quick recovery. This aligns with our finding that soon after re-wetting drought intensity no longer affected GPP (Figure S4). Only 10 days after re-wetting, there was evidence of GPP over-compensatory effects in fast-strategy communities that had experienced the highest drought intensities, and this was maintained until the end of the

experiment. We show that the GPP overcompensation responses to drought depend on drought intensity in the early recovery phase (Figure S4). This is in line with previous studies showing quick post-drought recovery in grasslands dominated by fast-growing plants (Ingrisch et al., 2018). In the slow-strategy community, past drought intensity maintained its effect on C uptake and allocation to roots (Figure 2). In both communities, there was a shift to allocating more recently acquired C to EOC and microbial biomass C (Figure 2), and this was clearest in the slow community where increasing drought intensity reduced the relative amount of C partitioned to leaves in favour of partitioning it to microbial biomass and EOC (Figure S8). This shift in plant/soil C dynamics with increasing drought intensity may have contributed to plant community recovery. Increasing C allocation to EOC and microbial biomass reflects increased rhizodeposition and uptake by the microbial community, which could increase N availability in the rhizosphere (Henneron, Fontaine, et al., 2020; Henneron, Kardol, et al., 2020), as discussed below. Nine days after re-wetting, the microbial community had largely recovered in terms of ^{13}C incorporation into NLFA/PLFAs. However, ^{13}C incorporation into the NLFA representing AMF decreased with past drought intensity in both plant communities. Previous studies have found that while C allocation to the NLFA representing AMF quickly recovered after drought in a grassland dominated by fast-strategy plants, it remained lower plant communities dominated by slow-strategy plants (Karlowsky, Augusti, Ingrisch, Hasibeder, et al., 2018).

4.2.3 | Plant/soil N dynamics

We found that drought altered plant/soil N dynamics (Figure 4; Figures S9 and S10), which could play a key role in post-drought productivity overcompensation (Figure 1). Twelve days after re-wetting, leaf N concentration increased with past drought intensity in both plant communities, and the relationship was stronger in the fast community (Figure 4). Whole plant N uptake ($g\,N\,m^{-2}$) increased with increasing past drought intensity in the fast-strategy community only, while the slow-strategy community was not affected (Figure S10C). Thus, while leaf N concentration increased in both the fast- and slow-strategy plant communities with increasing past drought intensity, only the fast-strategy community increased its plant N uptake, signalling fast drought recovery. This supports our hypothesis that the fast-strategy community is more efficient in increasing N uptake soon after re-wetting. The increase in leaf N concentration and plant N uptake with past drought intensity could result from two sources of N: higher plant-available N in the soil (i.e. NO_3^--N, NH_4^+-N, Figure S9), and/or remobilization of root N stored during drought in the fast community (Figure 4).

An increase in soil NO_3^--N upon re-wetting after drought is frequently reported (e.g. Mackie et al., 2018; Roy et al., 2016) but has rarely been studied in response to increasing drought intensity. An increase in organic N sources via dead plant material and lysed microbial cells above a drought intensity of 75% SWD likely caused the increase in NH_4^+-N at peak drought, fuelling nitrification and the increase in NO_3^--N after the drought (Figure S9). Apart from microbial N transformation processes, this increase in N availability post-drought could be due to an increase in rhizodeposition with increasing drought intensity (discussed above). The more pronounced increase in leaf N concentration and whole plant N uptake with increasing drought intensity in the fast-strategy community only is consistent with earlier studies showing fast-strategy plants have higher rates of N uptake compared to slow-strategy plants (de Vries & Bardgett, 2016; Grassein et al., 2015). This facilitates a tighter coupling of C and N dynamics in the rhizosphere by accelerating N cycling via the input of labile C (Henneron, Fontaine, et al., 2020; Henneron, Kardol, et al., 2020). In the context of disturbance, fast-strategy plants may be specifically suited to recover quickly because they are able to take advantage of pulses of nutrients (Grime, 1979) caused by the Birch effect (Birch, 1958) upon re-wetting dry soil. Our findings are in line with this, as we found that although plant-available soil N increased with increasing drought intensity in both plant communities, the whole-plant N uptake increased in the fast- but not the slow-strategy plant community (Figure S10C). The contribution of a second N source in the fast community (re-mobilization of N stored in roots at peak drought) may have also contributed to its higher productivity overshoot and increased above-ground N pool, as storage of N in roots during stress and re-mobilization to leaves is an important factor for plant recovery (Masclaux-Daubresse et al., 2010).

5 | CONCLUSIONS

By implementing a gradient design in outdoor mesocosms, we show that grassland responses to drought intensity are non-linear at peak drought and during recovery. Advancing on previous work based on monocultures, we also discovered that productivity thresholds differed with plant community resource strategy: slow-strategy communities were more drought resistant than fast-strategy communities, but fast-strategy communities recovered faster and had a higher degree of overshoot after re-wetting. We also found that drought intensity governed below-ground C allocation and N dynamics in fast and slow communities at peak drought, while plant community strategy modulated recovery dynamics after rewetting. Collectively, our results highlight the role of drought intensity in understanding grassland ecosystem functioning during and after drought, and suggest that increasing drought intensity can trigger major functional shifts in grasslands that affect plant community recovery trajectories and have potential long-lasting effects (Müller & Bahn, 2022).

AUTHOR CONTRIBUTIONS

Natalie J. Oram and Johannes Ingrisch contributed equally and share first authorship. Natalie J. Oram, Michael Bahn, Johannes Ingrisch, Richard D. Bardgett and Fiona Brennan designed the study. Data collection was carried out by Natalie J. Oram, Johannes Ingrisch, Georg Dittmann, Gerd Gleixner, Nadine Praeg, Paul Illmer,

statistical analysis by Natalie J. Oram and Johannes Ingrisch, and the manuscript was written by Natalie J. Oram and Johannes Ingrisch with extensive input on data interpretation and writing from Michael Bahn, as well as Richard D. Bardgett, Fiona Brennan, Georg Dittmann, Gerd Gleixner, Nadine Praeg and Paul Illmer.

ACKNOWLEDGEMENTS

Authors would like to thank Laura Dobrowz, Thea Schwingshackl, Moritz Mairl, Greta Ploner, Dina in 't Zandt, Lena Müller, Akira Yoshikawa, Fabrizzio Protti, Deniz Scheerer, Suzanne Guyard, Andrew Giunta, Kathiravan Mohamed Meeran and Beverley Anderson who made this experiment possible and also a lot of fun. Thanks to Heike Geilmann for ^{13}C analysis of the leaves and roots, Anna Reichstein for ^{13}C analysis of TOC and EOC, and Stefan Karlowsky for helpful advice. Thank you to Barenbrug BV, the Netherlands for providing seeds for the experiment. NJO has received funding from the Research Leaders 2025 programme co-funded by Teagasc and the European Union's Horizon 2020 research and innovation programme under the Marie Sklowdowska-Curie grant agreement number 754380. RDB acknowledges support from a European Research Council (ERC) Advanced Grant (883621, SoilResist). The experiment was also supported by a Tiroler Wissenschaftsfonds grant to JI (grant ID F.16568/5-2019).

CONFLICT OF INTEREST STATEMENT

The authors declare no conflict of interest. Richard Bardgett is the Executive Editor of *Journal of Ecology*, but took no part in the peer review or decision-making process for this manuscript.

DATA AVAILABILITY STATEMENT

Data are available on Dryad Digital Repository https://doi.org/10.5061/dryad.5qfttdzbb (Oram, 2023).

ORCID

Natalie J. Oram https://orcid.org/0000-0002-3529-5166
Johannes Ingrisch https://orcid.org/0000-0002-8461-8689
Richard D. Bardgett https://orcid.org/0000-0002-5131-0127
Gerd Gleixner https://orcid.org/0000-0002-4616-0953
Paul Illmer https://orcid.org/0000-0003-3368-3015
Nadine Praeg https://orcid.org/0000-0002-1531-8543
Michael Bahn https://orcid.org/0000-0001-7482-9776

REFERENCES

Abalos, D., Groenigen, J. W., Philippot, L., Lubbers, I. M., & De Deyn, G. B. (2019). Plant trait-based approaches to improve nitrogen cycling in agroecosystems. *Journal of Applied Ecology*, *56*(11), 1–13. https://doi.org/10.1111/1365-2664.13489

Baxendale, C., Orwin, K. H., Poly, F., Pommier, T., & Bardgett, R. D. (2014). Are plant–soil feedback responses explained by plant traits? *New Phytologist*, *204*(2), 408–423. https://doi.org/10.1111/nph.12915

Berdugo, M., Delgado-baquerizo, M., Soliveres, S., Zhao, Y., Gross, N., Saiz, H., Maire, V., Lehmann, A., Rillig, M. C., & Maestre, F. T. (2020). Global ecosystem thresholds driven by aridity. *Science*, *790*(March), 787–790.

Birch, H. F. (1958). The effect of soil drying on humus decomposition and nitrogen availability. *Plant Soil*, *10*, 9–31.

Bligh, E. G., & Dyer, W. J. (1959). A rapid method of total lipid extraction and purification. *Canadian Journal of Biochemistry and Physiology*, *37*(8), 911–917. https://doi.org/10.1139/o59-099

Blumenthal, D. M., Mueller, K. E., Kray, J. A., Ocheltree, T. W., Augustine, D. J., & Wilcox, K. R. (2020). Traits link drought resistance with herbivore defence and plant economics in semi-arid grasslands: The central roles of phenology and leaf dry matter content. *Journal of Ecology*, *108*(6), 2336–2351. https://doi.org/10.1111/1365-2745.13454

Canarini, A., Schmidt, H., Fuchslueger, L., Martin, V., Herbold, C. W., Zezula, D., Gündler, P., Hasibeder, R., Jecmenica, M., Bahn, M., & Richter, A. (2021). Ecological memory of recurrent drought modifies soil processes via changes in soil microbial community. *Nature Communications*, *12*(1), 1–14. https://doi.org/10.1038/s41467-021-25675-4

Chomel, M., Baggs, E. M., Lavallee, J. M., Caruso, T., Alvarez, N., Francisco, S., Vries, F. T. D., Rhymes, J. M., Emmerson, M. C., Bardgett, R. D., & Johnson, D. (2019). Drought decreases incorporation of recent plant photosynthate into soil food webs regardless of their trophic complexity. *Global Change Biology*, *25*, 3549–3561. https://doi.org/10.1111/gcb.14754

Chomel, M., Lavallee, J. M., Alvarez-segura, N., Baggs, E. M., Caruso, T., De Castro, F., Emmerson, M. C., Magilton, M., Rhymes, J. M., De Vries, F. T., Johnson, D., & Bardgett, R. D. (2022). Intensive grassland management disrupts below-ground multi-trophic resource transfer in response to drought. *Nature Communications*, *1–12*, *6991*. https://doi.org/10.1038/s41467-022-34449-5

De Long, J. R., Jackson, B. G., Wilkinson, A., Pritchard, W. J., Oakley, S., Mason, K. E., Stephan, J. G., Ostle, N. J., Johnson, D., Baggs, E. M., & Bardgett, R. D. (2019). Relationships between plant traits, soil properties and carbon fluxes differ between monocultures and mixed communities in temperate grassland. *Journal of Ecology*, *November 2018*, 1–16. https://doi.org/10.1111/1365-2745.13160

de Vries, F. T., & Bardgett, R. D. (2016). Plant community controls on short-term ecosystem nitrogen retention. *New Phytologist*, *210*(3), 861–874. https://doi.org/10.1111/nph.13832

Díaz, S., Kattge, J., Cornelissen, J. H. C., Wright, I. J., Lavorel, S., Dray, S., Reu, B., Kleyer, M., Wirth, C., Colin Prentice, I., Garnier, E., Bönisch, G., Westoby, M., Poorter, H., Reich, P. B., Moles, A. T., Dickie, J., Gillison, A. N., Zanne, A. E., … Gorné, L. D. (2016). The global spectrum of plant form and function. *Nature*, *529*(7585), 167–171. https://doi.org/10.1038/nature16489

Fong, Y., Huang, Y., Gilbert, P. B., & Permar, S. R. (2017). chngpt: Threshold regression model estimation and inference. *BMC Bioinformatics*, *18*(1), 1–7. https://doi.org/10.1186/s12859-017-1863-x

Freschet, G. T., Aerts, R., & Cornelissen, J. H. C. (2012). A plant economics spectrum of litter decomposability. *Functional Ecology*, *26*(1), 56–65. https://doi.org/10.1111/j.1365-2435.2011.01913.x

Frostegård, A., & Bååth, E. (1996). The use of phospholipid fatty acid analysis to estimate bacterial and fungal biomass in soil. *Biology and Fertility of Soils*, *22*(1–2), 59–65. https://doi.org/10.1007/s003740050076

Fuchslueger, L., Bahn, M., Fritz, K., Hasibeder, R., & Richter, A. (2014). Experimental drought reduces the transfer of recently fixed plant carbon to soil microbes and alters the bacterial community composition in a mountain meadow. *New Phytologist*, *201*(3), 916–927. https://doi.org/10.1111/nph.12569

Grassein, F., Lemauviel-Lavenant, S., Lavorel, S., Bahn, M., Bardgett, R. D., Desclos-Theveniau, M., & Laîné, P. (2015). Relationships between functional traits and inorganic nitrogen acquisition among

eight contrasting European grass species. *Annals of Botany*, *115*(1), 107–115. https://doi.org/10.1093/aob/mcu233

Grime, J. P. (1977). Evidence for the existence of three primary strategies in plants and its relevance to ecological and evolutionary theory. *The American Naturalist*, *111*(982), 1169–1194.

Grime, J. P. (1979). *Plant strategies, vegetation processes, and ecosystem properties*. John Wiley & Sons Ltd.

Grime, J. P., Brown, V. K., Thompson, K., Masters, G. J., Hillier, S. H., Clarke, I. P., Askew, A. P., Corker, D., & Kielty, J. P. (2000). The response of two contrasting limestone grasslands to simulated climate change. *Science*, *289*(5480), 762–765. https://doi.org/10.1126/science.289.5480.762

Grime, J. P., & Mackey, J. M. L. (2002). The role of plasticity in resource capture by plants. *Evolutionary Ecology*, *16*(3), 299–307. https://doi.org/10.1023/A:1019640813676

Groffman, P. M., Baron, J. S., Blett, T., Gold, A. J., Goodman, I., Gunderson, L. H., Levinson, B. M., Palmer, M. A., Paerl, H. W., Peterson, G. D., Poff, N. L. R., Rejeski, D. W., Reynolds, J. F., Turner, M. G., Weathers, K. C., & Wiens, J. (2006). Ecological thresholds: The key to successful environmental management or an important concept with no practical application? *Ecosystems*, *9*(1), 1–13. https://doi.org/10.1007/s10021-003-0142-z

Grünzweig, J. M., De Boeck, H. J., Rey, A., Santos, M. J., Adam, O., Bahn, M., Belnap, J., Deckmyn, G., Dekker, S. C., Flores, O., Gliksman, D., Helman, D., Hultine, K. R., Liu, L., Meron, E., Michael, Y., Sheffer, E., Throop, H. L., Tzuk, O., & Yakir, D. (2022). Dryland mechanisms could widely control ecosystem functioning in a drier and warmer world. *Nature Ecology and Evolution*, *6*(8), 1064–1076. https://doi.org/10.1038/s41559-022-01779-y

Hafner, S., Unteregelsbacher, S., Seeber, E., Lena, B., Xu, X., Li, X., Guggenberger, G., Miehe, G., & Kuzyakov, Y. (2012). Effect of grazing on carbon stocks and assimilate partitioning in a Tibetan montane pasture revealed by $^{13}CO_2$ pulse labeling. *Global Change Biology*, *18*(2), 528–538. https://doi.org/10.1111/j.1365-2486.2011.02557.x

Hartmann, H., Bahn, M., Carbone, M., & Richardson, A. D. (2020). Plant carbon allocation in a changing world—Challenges and progress: Introduction to a Virtual Issue on carbon allocation. *New Phytologist*, *227*(4), 981–988. https://doi.org/10.1111/nph.16757

Hasibeder, R., Fuchslueger, L., Richter, A., & Bahn, M. (2015). Summer drought alters carbon allocation to roots and root respiration in mountain grassland. *New Phytologist*, *205*(3), 1117–1127. https://doi.org/10.1111/nph.13146

Henneron, L., Fontaine, S., Cros, C., Picon, C., & Vida, C. (2020). Plant economic strategies of grassland species control soil carbon dynamics through rhizodeposition. *Journal of Ecology*, *108*, 528–545. https://doi.org/10.1111/1365-2745.13276

Henneron, L., Kardol, P., Wardle, D. A., Cros, C., & Fontaine, S. (2020). Rhizosphere control of soil nitrogen cycling: A key component of plant economic strategies. *New Phytologist*, *228*(4), 1269–1282. https://doi.org/10.1111/nph.16760

Hillebrand, H., Donohue, I., Harpole, W. S., Hodapp, D., Kucera, M., Lewandowska, A. M., Merder, J., Montoya, J. M., & Freund, J. A. (2020). Thresholds for ecological responses to global change do not emerge from empirical data. *Nature Ecology and Evolution*, *4*(11), 1502–1509. https://doi.org/10.1038/s41559-020-1256-9

Ingrisch, J., Karlowsky, S., Anadon-Rosell, A., Hasibeder, R., König, A., Augusti, A., Gleixner, G., & Bahn, M. (2018). Land use alters the drought responses of productivity and CO_2 fluxes in mountain grassland. *Ecosystems*, *21*(4), 689–703. https://doi.org/10.1007/s10021-017-0178-0

Ingrisch, J., Karlowsky, S., Hasibeder, R., Gleixner, G., & Bahn, M. (2020). Drought and recovery effects on belowground respiration dynamics and the partitioning of recent carbon in managed and abandoned grassland. *Global Change Biology*, *26*(8), 4366–4378. https://doi.org/10.1111/gcb.15131

Ingrisch, J., Umlauf, N., & Bahn, M. (2023). Functional thresholds alter the relationship of plant resistance and recovery to drought. *Ecology*, *104*(2), 1–15. https://doi.org/10.1002/ecy.3907

IPCC. (2021). *Climate change 2021: The physical science basis. Contribution of Working Group I to the sixth assessment report of the Intergovernmental Panel on Climate Change* [V. Masson-Delmotte, P. Zhai, A. Pirani, S. Connors, C. Péan, S. Berger, N. Caud, Y. Chen, L. Goldfarb, M. Gomis, M. Huang, K. Leitzell, E. Lonnoy, J. Matthews, T. Maycock, T. Waterfield, O. Yelekçi, R. Yu, & B. Zhou (Eds.)]. Cambridge University Press.

Jia, Y., van der Heijden, M. G. A., Wagg, C., Feng, G., & Walder, F. (2020). Symbiotic soil fungi enhance resistance and resilience of an experimental grassland to drought and nitrogen deposition. *Journal of Ecology*, *May*, 1–11. https://doi.org/10.1111/1365-2745.13521

Karlowsky, S., Augusti, A., Ingrisch, J., Akanda, M. K. U., Bahn, M., & Gleixner, G. (2018). Drought-induced accumulation of root exudates supports post-drought recovery of microbes in mountain grassland. *Frontiers in Plant Science*, *9*(November), 1–16. https://doi.org/10.3389/fpls.2018.01593

Karlowsky, S., Augusti, A., Ingrisch, J., Hasibeder, R., Lange, M., Lavorel, S., Bahn, M., & Gleixner, G. (2018). Land use in mountain grasslands alters drought response and recovery of carbon allocation and plant-microbial interactions. *Journal of Ecology*, *106*(3), 1230–1243. https://doi.org/10.1111/1365-2745.12910

Kaštovská, E., Edwards, K., Picek, T., & Šantrůčková, H. (2015). A larger investment into exudation by competitive versus conservative plants is connected to more coupled plant–microbe N cycling. *Biogeochemistry*, *122*(1), 47–59. https://doi.org/10.1007/s10533-014-0028-5

Kreyling, J., Schweiger, A. H., Bahn, M., Ineson, P., Migliavacca, M., Morel-Journel, T., Christiansen, J. R., Schtickzelle, N., & Larsen, K. S. (2018). To replicate, or not to replicate—That is the question: How to tackle nonlinear responses in ecological experiments. *Ecology Letters*, *21*, 1629–1638. https://doi.org/10.1111/ele.13134

Le, S., Josse, J., & Husson, F. (2008). FactoMineR: An R package for multivariate analysis. *Journal of Statistical Software*, *25*(1), 1–18. https://doi.org/10.18637/jss.v025.i01

Lechevalier, M. P., De Bievre, C., & Lechevalier, H. (1977). Chemotaxonomy of aerobic actinomycetes: Phospholipid composition. *Biochemical Systematics and Ecology*, *5*(4), 249–260. https://doi.org/10.1016/0305-1978(77)90021-7

Legay, N., Baxendale, C., Grigulis, K., Krainer, U., Kastl, E., Schloter, M., Bardgett, R. D., Arnoldi, C., Bahn, M., Dumont, M., Poly, F., Pommier, T., Clément, J. C., & Lavorel, S. (2014). Contribution of above- and below-ground plant traits to the structure and function of grassland soil microbial communities. *Annals of Botany*, *114*, 1011–1021. https://doi.org/10.1093/aob/mcu169

Lepš, J., Osbornová-Kosinová, J., & Rejmánek, M. (1982). Community stability, complexity and species life history strategies. *Vegetatio*, *50*(1), 53–63. https://doi.org/10.1007/BF00120678

Lind, E. M., Borer, E., Bakker, J. D., Crawley, M., Davies, K., & Harpole, W. S. (2013). Life-history constraints in grassland plant species: A growth-defence trade-off is the norm. *Ecology Letters*, *16*, 513–521. https://doi.org/10.1111/ele.12078

Mackie, K. A., Zeiter, M., Bloor, J. M. G., & Stampfli, A. (2018). Plant functional groups mediate drought resistance and recovery in a multisite grassland experiment. *Journal of Ecology*, *107*(November 2018), 937–949. https://doi.org/10.1111/1365-2745.13102

Masclaux-Daubresse, C., Daniel-Vedele, F., Dechorgnat, J., Chardon, F., Gaufichon, L., & Suzuki, A. (2010). Nitrogen uptake, assimilation and remobilization in plants: Challenges for sustainable and productive agriculture. *Annals of Botany*, *105*(7), 1141–1157. https://doi.org/10.1093/aob/mcq028

Mellado-Vázquez, P. G., Lange, M., Bachmann, D., Gockele, A., Karlowsky, S., Milcu, A., Piel, C., Roscher, C., Roy, J., & Gleixner, G. (2016). Plant diversity generates enhanced soil microbial access to

recently photosynthesized carbon in the rhizosphere. *Soil Biology and Biochemistry*, *94*, 122–132. https://doi.org/10.1016/j.soilbio.2015.11.012

Müller, L. M., & Bahn, M. (2022). Drought legacies and ecosystem responses to subsequent drought. *Global Change Biology*, *28*(17), 5086–5103. https://doi.org/10.1111/gcb.16270

Naylor, D., Degraaf, S., Purdom, E., & Coleman-Derr, D. (2017). Drought and host selection influence bacterial community dynamics in the grass root microbiome. *ISME Journal*, *11*(12), 2691–2704. https://doi.org/10.1038/ismej.2017.118

Oliveira, R. S., Eller, C. B., de Barros, F. V., Hirota, M., Brum, M., & Bittencourt, P. (2021). Linking plant hydraulics and the fast–slow continuum to understand resilience to drought in tropical ecosystems. *New Phytologist*, *230*(3), 904–923. https://doi.org/10.1111/nph.17266

Olsson, P. A. (1999). Signature fatty acids provide tools for determination of the distribution and interactions of mycorrhizal fungi in soil. *FEMS Microbiology Ecology*, *29*(4), 303–310. https://doi.org/10.1016/S0168-6496(99)00021-5

Oram, N. (2023). Drought intensity alters productivity, carbon allocation, and plant nitrogen uptake in fast versus slow grassland communities, Dryad, Dataset. https://doi.org/10.5061/dryad.5qfttdzbb

Padullés Cubino, J., Axmanová, I., Lososová, Z., Večeřa, M., Bergamini, A., Bruelheide, H., Dengler, J., Jandt, U., Jansen, F., Pätsch, R., & Chytrý, M. (2022). The effect of niche filtering on plant species abundance in temperate grassland communities. *Functional Ecology*, *36*(4), 962–973. https://doi.org/10.1111/1365-2435.13994

Pantigoso, H. A., Newberger, D., & Vivanco, J. M. (2022). The rhizosphere microbiome: Plant–microbial interactions for resource acquisition. *Journal of Applied Microbiology*, *133*(5), 2864–2876. https://doi.org/10.1111/jam.15686

Pedersen, T. L. (2020). *patchwork: The composer of plots*. (R package version 1.1.1). https://cran.r-project.org/package=patchwork

Pérez Castro, S., Cleland, E. E., Wagner, R., Al Sawad, R., & Lipson, D. A. (2019). Soil microbial responses to drought and exotic plants shift carbon metabolism. *ISME Journal*, *13*(7), 1776–1787. https://doi.org/10.1038/s41396-019-0389-9

Pérez-Harguindeguy, N., Díaz, S., Garnier, E., Lavorel, S., Poorter, H., Jaureguiberry, P., Bret-Harte, M., Cornwell, W., Craine, J., Gurvich, D., Urcelay, C., Veneklaas, E., Reich, P., Poorter, L., Wright, I., Ray, P., Enrico, L., Pausas, J., de Vos, A., … Cornelissen, J. (2016). New handbook for standardised measurement of plant functional traits worldwide. *Australian Journal of Botany*, *61*, 167–234.

Pérez-Ramos, I. M., Volaire, F., Fattet, M., Blanchard, A., & Roumet, C. (2013). Tradeoffs between functional strategies for resource-use and drought-survival in Mediterranean rangeland species. *Environmental and Experimental Botany*, *87*, 126–136. https://doi.org/10.1016/j.envexpbot.2012.09.004

Pérez-Ramos, I. M., Roumet, C., Cruz, P., Blanchard, A., Autran, P., & Garnier, E. (2012). Evidence for a 'plant community economics spectrum' driven by nutrient and water limitations in a Mediterranean rangeland of southern France. *Journal of Ecology*, *100*(6), 1315–1327. https://doi.org/10.1111/1365-2745.12000

R Core Team. (2020). *R: A language and environment for statistical computing*. R Foundation for Statistical Computing. https://www.r-project.org/

Reich, P. B. (2014). The world-wide 'fast-slow' plant economics spectrum: A traits manifesto. *Journal of Ecology*, *102*(2), 275–301. https://doi.org/10.1111/1365-2745.12211

Reichstein, M., Bahn, M., Ciais, P., Frank, D., Mahecha, M. D., Seneviratne, S. I., Zscheischler, J., Beer, C., Buchmann, N., Frank, D. C., Papale, D., Rammig, A., Smith, P., Thonicke, K., Van Der Velde, M., Vicca, S., Walz, A., & Wattenbach, M. (2013). Climate extremes and the carbon cycle. *Nature*, *500*(7462), 287–295. https://doi.org/10.1038/nature12350

Roy, J., Picon-Cochard, C., Augusti, A., Benot, M. L., Thiery, L., Darsonville, O., Landais, D., Piel, C., Defossez, M., Devidal, S., Escape, C., Ravel, O., Fromin, N., Volaire, F., Milcu, A., Bahn, M., & Soussana, J.-F. (2016). Elevated CO_2 maintains grassland net carbon uptake under a future heat and drought extreme. *Proceedings of the National Academy of Sciences of the United States of America*, *113*(22), 6224–6229. https://doi.org/10.1073/pnas.1524527113

Rudgers, J. A., Afkhami, M. E., Bell-Dereske, L., Chung, Y. A., Crawford, K. M., Kivlin, S. N., Mann, M. A., & Nuntildez, M. A. (2020). Climate disruption of plant-microbe interactions. *Annual Review of Ecology, Evolution, and Systematics*, *51*, 561–586. https://doi.org/10.1146/annurev-ecolsys-011720-090819

Sanaullah, M., Chabbi, A., Rumpel, C., & Kuzyakov, Y. (2012). Carbon allocation in grassland communities under drought stress followed by ^{14}C pulse labeling. *Soil Biology and Biochemistry*, *55*, 132–139. https://doi.org/10.1016/j.soilbio.2012.06.004

Scheibe, A., Krantz, L., & Gleixner, G. (2012). Simultaneous determination of the quantity and isotopic signature of dissolved organic matter from soil water using high-performance liquid chromatography/isotope ratio mass spectrometry. *Rapid Communications in Mass Spectrometry*, *26*(2), 173–180. https://doi.org/10.1002/rcm.5311

Schinner, F., Öhlinger, R., Kandeler, E., & Margesin, R. (1996). *Methods in soil biology*. Springer.

Seeber, J., Rief, A., Richter, A., Traugott, M., & Bahn, M. (2012). Drought-induced reduction in uptake of recently photosynthesized carbon by springtails and mites in alpine grassland. *Soil Biology and Biochemistry*, *55*, 37–39. https://doi.org/10.1016/j.soilbio.2012.06.009

Sippel, S., Reichstein, M., Ma, X., Mahecha, M. D., Lange, H., Flach, M., & Frank, D. (2018). Drought, heat, and the carbon cycle: A review. *Current Climate Change Reports*, *4*(3), 266–286. https://doi.org/10.1007/s40641-018-0103-4

Spitzer, C. M., Lindahl, B., Wardle, D. A., Sundqvist, M. K., Gundale, M. J., Fanin, N., & Kardol, P. (2021). Root trait–microbial relationships across tundra plant species. *New Phytologist*, *229*(3), 1508–1520. https://doi.org/10.1111/nph.16982

Taketani, R. G., Lançoni, M. D., Kavamura, V. N., Durrer, A., Andreote, F. D., & Melo, I. S. (2017). Dry season constrains bacterial phylogenetic diversity in a semi-arid rhizosphere system. *Microbial Ecology*, *73*(1), 153–161. https://doi.org/10.1007/s00248-016-0835-4

Turner, M. G., Calder, W. J., Cumming, G. S., Hughes, T. P., Jentsch, A., LaDeau, S. L., Lenton, T. M., Shuman, B. N., Turetsky, M. R., Ratajczak, Z., Williams, J. W., Williams, A. P., & Carpenter, S. R. (2020). Climate change, ecosystems and abrupt change: Science priorities. *Philosophical Transactions of the Royal Society, B: Biological Sciences*, *375*(1794), 20190105. https://doi.org/10.1098/rstb.2019.0105

Vance, E. D., Brookes, P. C., & Jenkinson, D. S. (1987). An extraction method for measuring soil microbial biomass C. *Soil Biology and Biochemistry*, *19*(6), 703–707.

Volaire, F. (2018). A unified framework of plant adaptive strategies to drought: Crossing scales and disciplines. *Global Change Biology*, *24*(7), 2929–2938. https://doi.org/10.1111/gcb.14062

Voroney, R. P., Brookes, P. C., & Beyaert, R. P. (2007). Soil microbial biomass C, N, P and S. In M. R. Carter & E. G. Gregorich (Eds.), *Soil sampling and methods of analysis*. CRC Press, Taylor & Francis Group, LLC.

Wickham, H. (2016). *ggplot2: Elegant graphics for data analysis*. Springer-Verlag.

Wilcox, K. R., Blumenthal, D. M., Kray, J. A., Mueller, K. E., Derner, J. D., Ocheltree, T., & Porensky, L. M. (2021). Plant traits related to precipitation sensitivity of species and communities in semiarid shortgrass prairie. *New Phytologist*, *229*(4), 2007–2019. https://doi.org/10.1111/nph.17000

Wilke, C. O. (2019). *cowplot: Streamlined plot theme and plot annotations for 'ggplot2'*. (R package version 1.0.0). https://cran.r-project.org/package=cowplot

Williams, A., & de Vries, F. T. (2020). Plant root exudation under drought: Implications for ecosystem functioning. *New Phytologist*, *225*, 1899–1905. https://doi.org/10.1111/nph.16223

Wood, S. N. (2011). Fast stable restricted maximum likelihood and marginal likelihood estimation of semiparametric generalized linear models. *Journal of the Royal Statistical Society (B)*, *73*(1), 3–36.

Wu, Q. S. (2017). Arbuscular mycorrhizas and stress tolerance of plants. In *Arbuscular mycorrhizas and stress tolerance of plants* (pp. 1–327). https://doi.org/10.1007/978-981-10-4115-0

Xi, N., Adler, P. B., Chen, D., Wu, H., Catford, J. A., van Bodegom, P. M., Bahn, M., Crawford, K. M., & Chu, C. (2021). Relationships between plant–soil feedbacks and functional traits. *Journal of Ecology*, *109*(9), 3411–3423. https://doi.org/10.1111/1365-2745.13731

Zelles, L. (1997). Phospholipid fatty acid profiles in selected members of soil microbial communities. *Chemosphere*, *35*(1–2), 275–294. https://doi.org/10.1016/S0045-6535(97)00155-0

Zelles, L. (1999). Fatty acid patterns of phospholipids and lipopolysaccharides in the characterisation of microbial communities in soil: A review. *Biology and Fertility of Soils*, *29*(2), 111–129. https://doi.org/10.1007/s003740050533

SUPPORTING INFORMATION

Additional supporting information can be found online in the Supporting Information section at the end of this article.

Figure S1: The experiment consisted of five sets of mesocosms ($n = 210$). In sets 1–3, the control (20% soil water deficit) was replicated four times, and in sets 4 and 5 eight times to establish a dynamic baseline. Set 1 was used for the peak drought pulse-labelling campaign (eight drought intensities and a replicated [$n = 4$] control per plant community, $n = 24$), and an identical set (set 2) was used for the pulse labelling at early recovery. Set 3 was reserved for non-destructive measures (13 drought intensities and a replicated control [$n = 4$] per plant community strategy, n = 34). Finally, two sets of mesocosms destined for a follow-up study (sets 4 and 5) were included in the present study for non-destructive measurements (nine drought intensities and a replicated [$n = 8$] control, $n = 128$).

Figure S2: Dry-down dynamics. (A) Realized soil water deficit (SWD) indicates the actual SWD over time (day of the calendar year). The grey horizontal line at 20% realized SWD indicates the target control, the colours indicate the target SWD. (B) Relationship between realized and target SWD at peak drought (225 day of the calendar year). The diagonal dashed line indicates the 1:1 line, the solid black line is a linear regression, the R^2 indicates the adjusted R^2 of the linear regression between realized and target SWD.

Figure S3: (A) Microclimatic conditions throughout the experiment. Orange shaded area indicates the 3-week drought period, triangles indicate the dates of the $^{13}CO_2$ pulse labelling. During drought, all mesocosms were under a rain-out shelter and were watered according to their position on the drought intensity gradient to maintain their pre-defined soil water deficit. (B) Microclimatic conditions on the pulse-labelling days. The bars at the bottom indicate time and duration of the pulse labelling at peak drought and during recovery. Data from the climate station TAWES UIBK, provided by the Austrian Weather Service ZAMG (https://www.zamg.ac.at/cms/de/aktuell) and the Department of Atmospheric and Cryospheric Sciences, University of Innsbruck.

Figure S4: Gross primary productivity (GPP) across the drought intensity gradient over time. Increasing soil water deficit (percentage of field capacity) indicates a more intense drought. The drought began on 21 July 2020 and continued until 15 August 2020 when the mesocosms were re-wet to their control weight (20% SWD) over 3 days. The effect of soil water deficit on gross primary productivity, and whether this relationship depended on plant community (i.e. a fast or slow strategy) was determined using generalized additive models with soil water deficit and plant community (community) as fixed factors, and the interaction between soil water deficit and plant community. When a significant interaction occurred, a second model that tested the relationship between soil water deficit and gross primary productivity within each plant community was used. $p < 0.001^{***}$, $p < 0.01^{**}$, $p < 0.05^{*}$. R^2 adjusted indicates the explained variation of the GAM model, for full statistical output, see Table S6.

Figure S5: Normalized difference vegetation index (NDVI) across the drought intensity gradient over time. Increasing soil water deficit indicates a more intense drought. The drought began on 21 July 2020 and continued until 15 August 2020 when the mesocosms were re-wet to their control weight (20% soil water deficit) over 3 days. The effect of soil water deficit on NDVI, and whether this relationship depended on plant community (i.e. a fast or slow strategy), was determined using generalized additive models with soil water deficit and plant community (community) as fixed factors, and the interaction between soil water deficit and plant community. When a significant interaction occurred, a second model that tested the relationship between soil water deficit and NDVI within each plant community was used. $p < 0.001^{***}$, $p < 0.01^{**}$, $p < 0.05^{*}$. R^2 adjusted indicates the explained variation of the GAM model, for full statistical output, see Table S7.

Figure S6: Mean canopy height across the drought intensity gradient over time. Increasing soil water deficit indicates a more intense drought. The drought began on 21 July 2020 and continued until 15 August 2020 when the mesocosms were re-wet to their control weight (20% soil water deficit) over 3 days. The effect of soil water deficit on canopy height, and whether this relationship depended on plant community (i.e. a fast or slow strategy), was determined using generalized additive models with soil water deficit and plant community (community) as fixed factors, and the interaction between soil water deficit and plant community. When a significant interaction occurred, a second model that tested the relationship between soil water deficit and canopy height within each plant community was used. $p < 0.001^{***}$, $p < 0.01^{**}$, $p < 0.05^{*}$. R^2 adjusted indicates the explained variation of the GAM model, for full statistical output, see Table S8.

Figure S7: Relative partitioning of ^{13}C at three time points following the peak drought $^{13}CO_2$ pulse labelling. Relative partitioning is the percent of ^{13}C partitioned into leaves (A–C), roots (D–F), microbial biomass (G–I) and extractable organic carbon (J–L) relative to the total ^{13}C measured in all compartments immediately after labelling (*T0*). *p* values show the effect of soil water deficit (continuous),

plant community (ordered factor) and their interaction on the response variable based on a generalized additive model (GAM). If a significant interaction was found, a second GAM model was used to test the relationship between soil water deficit and the response variable within the fast and the slow strategy plant communities (see Section 2 for more information). $p < 0.001^{***}$, $p < 0.01^{**}$, $p < 0.05^{*}$. R^2 adjusted indicates the explained variation of the GAM model, for full statistical output, see Table S9.

Figure S8: Relative partitioning of ^{13}C at three time points following the early recovery $^{13}CO_2$ pulse labelling. Relative partitioning is the percent of ^{13}C partitioned into leaves (A–C), roots (D–F), microbial biomass (G–I) and extractable organic carbon (J–L) relative to the total ^{13}C measured in all compartments immediately after labelling (*T0*). *p* values show the effect of soil water deficit (continuous), plant community (ordered factor) and their interaction on the response variable based on a generalized additive model (GAM). If a significant interaction was found, a second GAM model was used to test the relationship between soil water deficit and the response variable within the fast and the slow strategy plant communities (see Section 2 for more information). $p < 0.001^{***}$, $p < 0.01^{**}$, $p < 0.05^{*}$. R^2 adjusted indicates the explained variation of the GAM model, for full statistical output, see Table S9.

Figure S9: Soil nitrogen and carbon at peak drought and early recovery (9 days after rewetting). $p < 0.001^{***}$, $p < 0.01^{**}$, $p < 0.05^{*}$. R^2 adjusted indicates the explained variation of the GAM model, for full statistical output, see Table S10.

Figure S10: (A) Whole plant nitrogen (N) pools at peak drought and (B) early recovery. Whole plant N pools are the sum of above-ground and below-ground N pools: N concentration ($g\,N\,g^{-1}$ plant tissue) multiplied by above-ground or below-ground biomass ($g\,m^{-2}$) at peak drought or early recovery. (C) Plant N uptake at early recovery is the N acquired during the first 12 days after re-wetting. $p < 0.001^{***}$, $p < 0.01^{**}$, $p < 0.05^{*}$. R^2 adjusted indicates the explained variation of the GAM model, for full statistical output, see Table S4.

Figure S11: The sum of ^{13}C incorporated into PLFAs and NLFAs representing microbial groups at (A) peak drought and (B) early recovery, 48 h after pulse labelling. Shaded areas indicate communities above the productivity threshold (Figure 1): fast-strategy communities in red, slow strategy in orange, and below the threshold: fast-strategy communities in dark blue, slow strategy in light blue.

Table S1: Leaf traits measured on plant species in the control treatment at the peak drought sampling campaign. Leaf dry matter content (LDMC), specific leaf area (SLA) and leaf nitrogen (N) concentration. Values indicate the mean of 3 or 4 replicates (denoted by n) ± the standard error of the mean.

Table S2: Mean CO_2 concentration and isotopic composition in the labelling chamber during the three pulse-labelling campaigns. Errors denote standard deviation.

Table S3: Statistical output of generalized additive models (GAMs) used to determine the effect of drought intensity (soil water deficit, SWD) and plant community strategy (fast or slow) on the ^{13}C incorporation into the measured compartments at the peak drought and early recovery pulse-labelling campaigns, directly (*T0*) and 120 h (*T5*) after labelling. Effective degrees of freedom (edf) denotes the linearity of the relationship (1.00 is linear), reference degrees of freedom (ref.df) and family that best fit the data distribution.

Table S4: Statistical output of generalized additive models (GAMs) used to determine the effect of drought intensity (soil water deficit, SWD) and plant community strategy (fast or slow) on the N concentration ($g\,N\,g^{-1}$ plant material), whole plant N pool ($g\,N\,m^{-2}$ ground area) at peak drought and early recovery, and whole plant N uptake ($g\,N\,m^{-2}$ ground area) at early recovery. Effective degrees of freedom (edf) denotes the linearity of the relationship (1.00 is linear), reference degrees of freedom (ref.df) and family that best fit the data distribution.

Table S5: Statistical output of generalized additive models (GAMs) used to determine the effect of drought intensity (soil water deficit, SWD) and plant community strategy (fast or slow) on ^{13}C incorporation into phospholipid fatty acids (PLFAs) and neutral lipid fatty acids (NLFA) representative of broad groups of bacteria and fungi. 13C incorporation was measured 48 h after pulse labelling at peak drought and early recovery. Effective degrees of freedom (edf) denotes the linearity of the relationship (1.00 is linear), reference degrees of freedom (ref.df) and family that best fit the data distribution.

Table S6: Statistical output of generalized additive models (GAMs) used to determine the effect of drought intensity (soil water deficit, SWD) and plant community strategy (fast or slow) on gross primary productivity (GPP) over time. Effective degrees of freedom (edf) denotes the linearity of the relationship (1.00 is linear), reference degrees of freedom (ref.df) and family that best fit the data distribution.

Table S7: Statistical output of generalized additive models (GAMs) used to determine the effect of drought intensity (soil water deficit, SWD) and plant community strategy (fast or slow) on NDVI over time. Effective degrees of freedom (edf) denotes the linearity of the relationship (1.00 is linear), reference degrees of freedom (ref.df) and family that best fit the data distribution.

Table S8: Statistical output of generalized additive models (GAMs) used to determine the effect of drought intensity (soil water deficit, SWD) and plant community strategy (fast or slow) on vegetative canopy height over time. Effective degrees of freedom (edf) denotes the linearity of the relationship (1.00 is linear), reference degrees of freedom (ref.df) and family that best fit the data distribution.

Table S9: Statistical output of generalized additive models (GAMs) used to determine the effect of drought intensity (soil water deficit, SWD) and plant community strategy (fast or slow) on the relative partitioning of ^{13}C at each pulse-labelling campaign. Relative partitioning is calculated as the absolute amount of ^{13}C in one compartment at one time point divided by the total uptake immediately after labelling (*T0*). ^{13}C incorporation was measured immediately (*T0*), 48 h (*T2*) and 120 h (*T5*) after pulse labelling. Effective degrees of freedom (edf) denotes the linearity of the relationship (1.00 is linear), reference degrees of freedom (ref.df) and family that best fit the data distribution.

Table S10: Statistical output of generalized additive models (GAMs) used to determine the effect of drought intensity (soil water deficit, SWD) and plant community strategy (fast or slow) on soil parameters. Abbreviations: total dissolved nitrogen (DN), nitrate (NO_3^-) and ammonium (NH_4^+). Effective degrees of freedom (edf) denotes the linearity of the relationship (1.00 is linear), reference degrees of freedom (ref.df) and family that best fit the data distribution.

Supplementary file S1: Materials and Methods.

How to cite this article: Oram, N. J., Ingrisch, J., Bardgett, R. D., Brennan, F., Dittmann, G., Gleixner, G., Illmer, P., Praeg, N., & Bahn, M. (2023). Drought intensity alters productivity, carbon allocation and plant nitrogen uptake in fast versus slow grassland communities. *Journal of Ecology*, *111*, 1681–1699. https://doi.org/10.1111/1365-2745.14136